ELSEVIER

Chemical Geology 142 (1997) 141–173

CHEMICAL GEOLOGY
INCLUDING
ISOTOPE GEOSCIENCE

Chemical and physical denudation in the Amazon River Basin

Jérôme Gaillardet [a,*], Bernard Dupré [b], Claude J. Allègre [c], Philippe Négrel [c]

[a] *Laboratoire de Géochimie et Cosmochimie, URA CNRS 1758, Institut de Physique du Globe, Université de Paris 7, 4 place Jussieu, 75252 Paris Cedex 05, France*

[b] *CNES / GRGS, 18 avenue E. Belin, 31055 Toulouse, France*

[c] *BRGM, Avenue de Concyr, 45000 Orléans, France*

Received 18 September 1996; revised 9 April 1997

Abstract

We present major and trace element data on the suspended and dissolved phases of the Amazon River and its main tributaries. The Sr isotopic composition of the dissolved load is also reported. Special attention is paid to the abundances of REE and to their fractionation between the dissolved and suspended phase. The rivers of the Amazon Basin are among the richest in dissolved REE and are similar to the rivers of the Congo system. However a greater range of fractionation between LREE and HREE is reported here. At a global scale the rivers have intermediate patterns between those of the Congo system and those of high pH rivers such as the Indus and Mississippi rivers. Only few elements (Rb, U, Ba, K, Na, Sr and Ca) are mobilized by silicate weathering. These elements are strongly depleted in the suspended phase with respect to upper continental crust. In the dissolved load, these elements are controlled by atmospheric inputs and the weathering of the main lithologies. We propose a model based on mass budget equations, that allow the proportions derived from the different sources to be calculated. As a consequence silicate, carbonate and evaporite weathering rates can be estimated as well as the consumption of CO_2 by weathering of each of these lithologies. Physical weathering rates can be estimated by two complementary approaches. On the one hand, the multi-year average of suspended sediments yields can be used to estimate physical denudation. On the other hand, we have developed a steady-state model of erosion that allows us to calculate physical erosion rates on the basis of the dissolved load of rivers. A mean crustal composition is assumed in this model for the rock sources of the drainage basins. Comparison of the rates predicted by the model to the observed rates shows good agreement for the lowland rivers, but a strong discrepancy for the rivers derived from the Andes. Andean rivers (Solimoes, Madeira and Amazon) have observed sediment yields much greater than those predicted according to the steady-state model of chemical and physical weathering. Two interpretations can account for this inconsistency. The first is that these rivers are not in steady state and hence that the soils are being destroyed. The second requires that the local continental crust is different from the average continental crust of Taylor and McLennan, and contains a large proportion of sedimentary rocks. Using the measured sediment yields, and assuming a steady state, we can estimate the amount of sediment recycling for each drainage basin. For the Amazon at Santarem, we find that at least 25% of the mass of the upper continental crust of the Amazon drainage basin is constituted of recycled material. © 1997 Elsevier Science B.V.

Keywords: Amazon River; Dissolved load; Suspended load; Trace elements; CO_2 consumption

* Corresponding author.

PII S0009-2541(97)00074-0

1. Introduction

Large rivers are a major pathway for the erosion products of continents to reach the oceans. Their study allows the erosion processes at a global scale to be addressed. In particular, geochemical investigation of large rivers gives important information about the biogeochemical cycles of the elements, weathering rates, physical erosion rates and CO_2 consumption by the acid degradation of continental rocks. A major challenge of the study of modern large rivers is to put some constraints on the input rates to the ocean of geochemical tracers used in oceanography and palaeoceanography.

Physical and chemical weathering, reflected in rivers as suspended sediments and dissolved matter, respectively, act together to denude the continents. Although good databases now exist for the major dissolved ion and dissolved organic carbon concentrations in the major world rivers (e.g. Degens et al., 1991), the chemistry of suspended solids transported by major rivers is poorly documented. A global tabulation of sediment chemistry of major rivers is given by Martin and Meybeck (1979). Only two large rivers have been investigated in details for major and trace elements in suspended sediments: the Orinoco River (Stallard et al., 1991) and the Congo River (Dupré et al., 1996). In addition, trace element systematics in the dissolved phase of large rivers are rather rare and incomplete (see e.g. Goldstein and Jacobsen (1988a) for a global tabulation of dissolved REE concentrations or Konhauser et al. (1994) for the Amazon River).

This paper is an attempt to fill in the gap in our knowledge of river-borne material chemistry and isotope chemistry and to link the chemical processes of erosion to the physical processes through the concept of steady state of erosion. This concept of equilibrium between production and export of solids through the entire drainage basin (Trimble, 1977), has rarely been considered in the literature on rivers. Papers attempting to relating physical and chemical weathering processes through the concept of stream equilibrium are Martin and Meybeck, 1979; Gaillardet et al., 1995; Stallard, 1995a, Stallard, 1995b; Allègre et al., 1996.

This paper focuses on the Amazon river system, the world's largest river in terms of water discharge. Major and trace element concentrations are reported for both dissolved and suspended phases. The isotopic composition of these phases has been published in a previous paper (Allègre et al., 1996).

With regard to dissolved ions and nutrients, the Amazon River is one of the most extensively documented in the world. Gibbs (1967), Stallard (1980), Stallard and Edmond (1983, Stallard and Edmond, 1987), Palmer and Edmond (1992) have measured major solutes, dissolved Fe, Al concentrations and Sr isotopic compositions for the Amazon mainstream and a number of tributaries. Seasonal variations of dissolved concentrations have been documented for the Solimoes by Devol et al. (1995) and for the Madeira River by Ferreira et al. (1988). Extensive databases have been set up over several years for concentrations of suspended solids transported in the Amazon (Meade, 1985; Richey et al., 1986; Guyot, 1993; Devol et al., 1995). As a consequence, the present-day sediment yields of the Amazon River are probably among the best known compared to other large rivers. The mineralogical composition of the Amazon River sediments has been reported by Gibbs (1967) and more recently by Irion (1983).

2. The Amazon river system

The Amazon river (6150 km length) is the largest river in the world in terms of water discharge (6300 km^3/yr) and drainage area ($6.15 \cdot 10^6$ km^2). It represents 15% of the total world runoff. The main tributaries are the Solimoes (accounting near Manaus for 56% of the total discharge of the Amazon at its mouth), the Rio Negro (16%), the Rio Madeira (17%), the Tapajos, Trombetas and Xingu (11%) according to Molinier et al. (1993). The discharge values for the Amazon and its tributaries are given in Table 8.

Following Stallard and Edmond (1983), the Amazon Basin can be divided in four major morphostructural units: the shields (Guayana Shield to the north, Brazilian Shield to the south), The central Amazon Trough, the Subandean area and the Western Andean Cordillera (Fig. 1). Among the major tributaries studied here, only the Rio Solimoes and Rio Madeira have their headwaters draining the Andean Cordillera, where altitudes often exceed 5000 m. Geologically,

the Andean Cordillera is very complex and composed of highly variable lithologic types.

– In the Solimoes Basin, the core of the Cordillera consists of the Precambrian basement, formed by sediments and igneous or metamorphic rocks. Palaeozoic and Mesozoic red beds, dark shales, and fractured carbonates are the main lithologies overlying the Precambrian basement. Evaporites (forming salt diapirs) are common rocks in the Maranon and Ucalayi drainages. Finally, the Andean Cordillera of the Solimoes Basin is characterized by a significant recent eruptive activity (Tertiary to the present). The lowland part of the Solimoes drainage consists of post-Palaeozoic and Tertiary fluvio-lacustrine sediments.

– By contrast, the Andean part of the Madeira drainage is more simple, consisting of lower Palaeozoic sediments associated with shales and rare Cam-

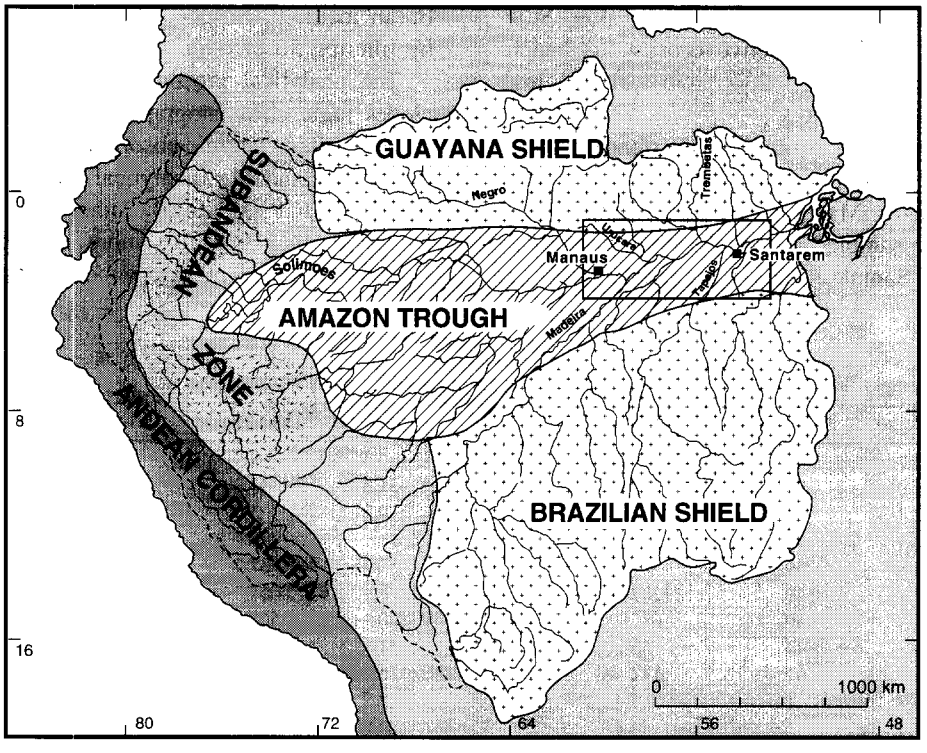

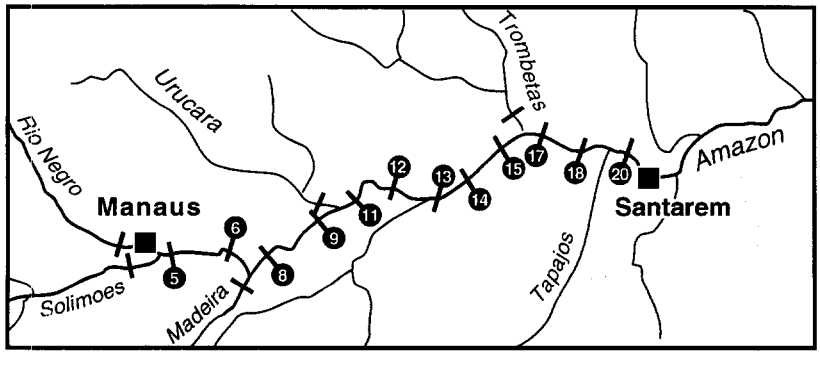

Fig. 1. Map of the Amazon River Basin showing the major geomorphological regions and the sampling locations between Manaus and Santarem. Samples were collected during the high-water stage of May 1989.

brian evaporites. The lower course of the Madeira, as that of the Solimoes, drains Tertiary fluvio-lacustrine sediments.

– The Rio Negro drains mainly the highly weathered Precambrian Shield and fluvio-lacustrine sediments in its lower course.

– Finally, The Trombetas and Tapajos rivers both have their headwaters in the elevated Shield terrains and drain the Palaeozoic sediments of the Amazon Trough.

The whole Amazon Basin is covered by tropical rainforest (71%) and savannas (29%, after Sioli, 1984). These highly productive ecosystems benefit from high rainfall (2000–2300 mm/yr) and high mean temperatures (25°C).

In this study, the Amazon mainstream between Manaus and Santarem, and the main tributaries (Solimoes, Negro, Madeira, Uracara, Trombetas and Tapajos) were sampled during the high water stage of May 1989. Sample locations are shown in Fig. 1.

3. Sampling and analytical methods

Samples are subsurface samples collected in acid-washed polypropylene containers. After collection, samples were filtered on site through 0.2 μm cellulose acetate filters (142 mm diameter) using a pressurized Sartorius® Teflon filtration unit. Filtered samples were stored in polypropylene acid-washed bottles and acidified with ultrapure HNO_3. The samples for anion determination were not acidified and the alkalinity was determined on site by acid titration (Gran method). Suspended sediments were isolated by filtering 5 l of river water.

The analytical procedure for water analysis includes ionic chromatography for Cl and SO_4, conventional flame atomic absorption spectrophotometry for Ca, Na and Mg (analytical precision better than 10%), and ICP–MS for the other trace elements (cf. Dupré et al., 1996, for more details). $^{87}Sr/^{86}Sr$ isotopic ratios were determined using mass spec-

Table 1
Concentrations (in ppm) in the suspended sediments of tributaries of the Amazon river

Sample	Rio Negro	Rio Solimoes	Rio Madeira	Urucara	Trombetas	Rio Tapajos	Congo mean	Upper Crust
Cs	3.7	8.6	15.0	3.7	3.4	9.3	4.8	3.7
Rb	24.0	92.0	79.0	46.0	31.8	43.2	69.5	112
U	2.4	4.1	3.9	2.7	4.3	3.5	2.9	2.8
Th	12.5	15.4	19.1	15.7		14.7	16.3	10.7
Pb	62.8	39.7	42	36.4	33.7	37.7	31	20
K	11977	17540	13267	11342	5276	6064	10415	28000
Ba	161	640	685	355	278	568	356	550
La	24	44	56	37	51	46	54	30
Ce	53	97	118	81	115	97	117	64
Ta	1.8	1.6	1.9	1.1	2.2	1.4	1.7	2.2
Hf	1.4	6.6	4.4	2.7	4.6	4.9	3.9	5.8
Nd	21.8	43.5	53.7	31.7	45		51	26
Zr		161	122		120	175	163	190
Sr	110	176	109	72	56	40	62	350
Na		12080	5729	2372	2149	7411	2547	28900
Sm	3.6	8.3	9.8	5.3	6.7	8.3	8.8	4.5
Eu	1.9	1.7	2.2	1.1	1.1	1.8	2	0.88
Tb	0.36	1	1.13	0.53	0.6	0.93	0.93	0.64
Yb	1.3	3.9	3.5	1.9	2.3	3.4	3.1	2.2
Sc	9.3	18.1	19.4	8.5	11.0	16.9	19.4	11
Fe	41423	55023	62639	92948	80591	59997	90708	35000
Co	8.1	21.1	18.0	11.1	7.4	16.4	25.9	10
Cr	52	77	88	99	79	86	134	35
Ni	69	55	43	20	14	37	85	20
pH	4.85	7.10	6.73	6.46	6.10	6.68		
TSS	5	53	67	8	13	6		

TSS: Total river suspended sediments in mg/l measured during the cruise.

Table 2
Concentrations (in ppm) in the suspended sediments of the Amazon mainstreams

Sample	Amazon 5 after Manaus	Amazon 6 before Madeira	Amazon 8 after Madeira	Amazon 9	Amazon 11	Amazon 12 before Parintins	Amazon 13	Amazon 14	Amazon 15	Amazon 17 after Obidos	Amazon 18 before Santarem	Amazon 20 after Santarem
Cs	7.9	10.4	11.8	10.8	10.3	10.5	10.4	10.6	11.1	10.5	10.4	11.7
Rb		94.0										44.0
U	3.7	3.7	3.8	3.5	3.5	3.1	3.5	3.7	3.9	3.7	3.6	3.9
Th	16.1	17.0	16.1	16.5	15.6	15.3	15.5	17.9	18.7	15.9	15.0	16.7
Pb		41.2		66.9								23.5
K		17156										5744
Ba	419	604	593	589	551	543	580	464	400	545	589	597
La	46	48	52	48	47	43	48	50	52	46	46	51
Ce	93	101	103	99	102	98	104	104	100	97	98	103
Ta	1.8	1.6	1.6	1.6	1.5	1.5	1.6	1.3	1.3	1.5	1.6	1.6
Hf	5.1	4.5	4.4	4.5	4.3	4.3	4.6	3.9	3.9	4.9	5.3	4.4
Nd		46.5										47.4
Zr	190	163	173	177	173	177	179	135	0	201	208	165
Sr		150										74
Na	5558	6492	6003	7122	6522	6225	6670	4447	4224	6966	7559	5632
Sm	7.3	8.5	9.4	8.1	8.2	8.9	8.2	9.2	9.0	8.5	8.3	9.1
Eu	1.8	2.1	1.9	1.8	2.0	1.8	1.8	1.9	1.6	1.8	1.9	1.9
Tb	0.74	1.04	1.01	0.91	0.98	0.93	0.96	1.04	0.93	0.97	0.98	0.98
Yb	2.9	3.6	3.7	3.2	3.4	3.5	3.5	3.7	3.5	3.6	3.6	3.7
Ca						5900						7600
Sc	16.1	18.9	17.7	18.0	17.2	17.4	17.2	16.5	17.0	17.6	17.8	18.6
Fe	54401	71110	59220	64893	67069	58909	61162	88285	88674	62173	54323	65515
Co	13.4	21.9	16.4	16.9	15.8	16.4	16.0	13.3	13.9	16.8	18.1	17.0
Cr	114	76	95	62	96	90	95	104	99	97	98	100
Ni	62	50	49	39	39	39	39	43	35	37	40	38
pH	5.77	6.79	6.78	6.81	6.60	6.75	6.86	7.06		6.78	6.86	6.89
TSS	7	36	43	19	28	36	8	6		25	95	34

TSS: Total river suspended sediments in mg/l measured during the cruise.

trometry. Sr, Rb and K concentrations were measured by isotope dilution with a ^{41}K, ^{87}Rb and ^{84}Sr spike (cf. Allègre et al., 1996 for more details).

The suspended sediments were separated from the cellulose acetate filters by scraping with Teflon tools. For isotopic measurements, the particles were transferred into a Teflon container and subjected to standard dissolution procedures in hot HCl, HNO_3, HF and $HClO_4$. An aliquot was then spiked with a ^{87}Rb, ^{84}Sr, ^{149}Sm and ^{150}Nd tracers. After chemical separation (Birck, 1986), Rb, Sr, Sm and Nd concentrations were determined by isotope dilution, mass spectrometry. Total blanks were negligible.

All other major and trace elements concentrations in suspended solids were measured using neutron activation as described in Dupré et al. (1996).

4. Results

4.1. Suspended load

Major and trace element compositions of suspended sediments are given Table 1 for the tributaries and Table 2 for the Amazon mainstream. The upper continental crust (UC) concentrations (Taylor and McLennan, 1985) and the mean composition of suspended material from the Congo river system (Dupré et al., 1996) are also given. The Sr–Nd–Pb isotopic composition of the suspended sediments can be found in Allègre et al. (1996).

4.1.1. Suspended sediments patterns

Absolute La concentrations range from 24 ppm in the sediments of the Rio Negro to 56 ppm in those of the Rio Madeira. All other REE are consistent with this range of variation as a result of their good intercorrelation coefficients. The low concentrations observed in the Rio Negro sediments are consistent with dilution of inorganic suspended material by organic material, first reported in the more particulate organic-rich rivers of the Congo Basin (Dupré et al., 1996).

The patterns of REE in suspended sediments normalized to UC concentrations are shown in Fig. 2a. Flat patterns are observed for the Solimoes, Madeira, Tapajos and Amazon mainstream. By contrast, the patterns of the Rio Negro, Urucara and Trombetas

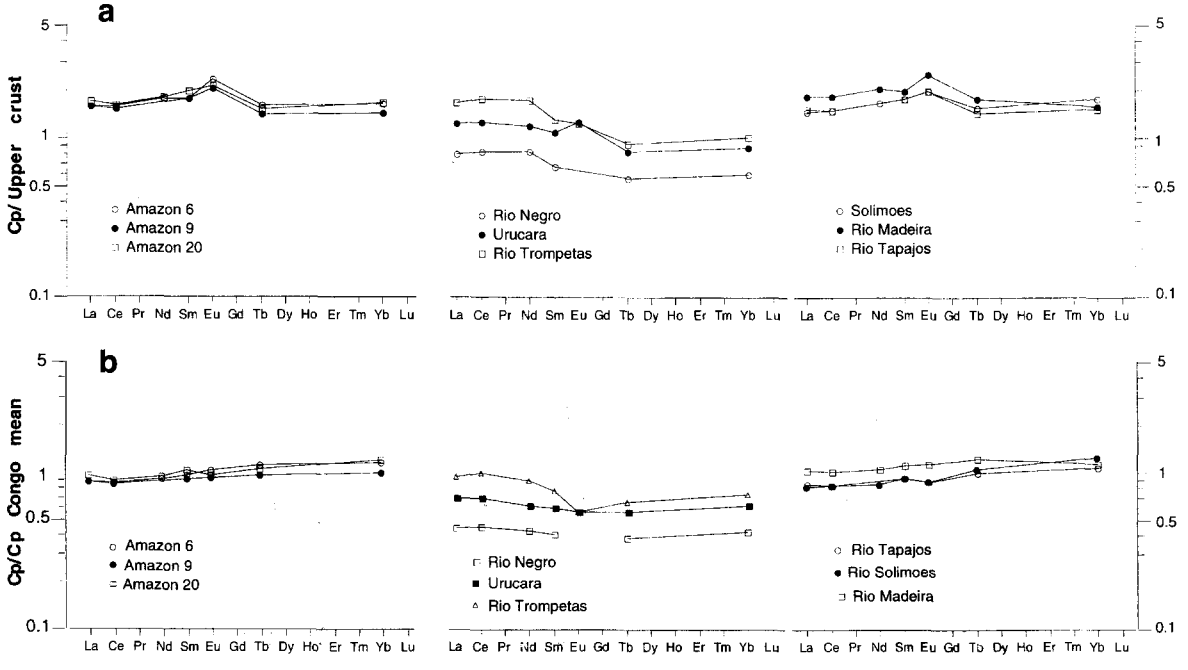

Fig. 2. REE patterns of the suspended sediments normalized (a) to the Upper Continental Crust (UC) of Taylor and McLennan (1985), and (b) to the mean composition of the suspended sediments of the Congo Basin rivers (Dupré et al., 1996). This normalization removes the slight positive Eu anomalies observed in the patterns of both Congo and Amazon sediments when normalized to UC.

are slightly LREE-enriched. A slight positive Eu anomaly is observed. When compared to the suspended sediments of the Congo river system (Fig. 2b), the suspended particles of the Amazon river system do not show any Eu anomaly. The La/Yb ratios of the Amazon river system normalized to the La/Yb ratio of suspended sediments of the Congo river system are greater than 1 for the Rio Negro (1.1), Urucara (1.1) and Trombetas (1.3), whereas the Rio Solimoes, Madeira, Tapajos and Amazon (20) have values lower than 1 (0.7, 0.9, 0.8, respectively). At its mouth, the Amazon (20) river is slightly depleted in LREE with respect to the particles of the Congo river (normalized La/Yb ratio is 0.8).

4.1.2. Extended diagrams

The UC normalized patterns for the whole set of elements are presented in Fig. 3. Such a representation has previously been used for the Congo Basin by Dupré et al. (1996). In such diagrams, the *X*-order of elements corresponds to the progressive enrichment from Ni to Cs of elements in the upper continental crust with respect to the primitive mantle of the Earth (Hofmann, 1988). This representation permits an overall examination of the data. Several observations are apparent from Fig. 3.

(1) The distinction pointed out for the Congo rivers between the elements Rb, U, Ba, K, Na, Sr and Ca and the other elements also exists for the Amazon rivers. The elements Rb, U, Ba, K, Na, Sr and Ca are considerably depleted in the suspended load with respect to the UC. As it has been shown by many authors (e.g. Nesbitt et al., 1980; Kronberg et al., 1987), these elements are the more mobile elements during the early stage of rock weathering. Fig. 3 confirms these conclusions and will allow us to quantify silicate weathering. Conversely, Cs, Th, Pb, REE, Ta, Sc, Fe, Co, Cr, Ni are slightly enriched and have, at a first order, UC-like patterns. Their enrichment with respect to the continental crust is due to the removal of the most soluble elements from the bedrock, which concentrates the remaining elements of lower solubility. Only the Rio Negro shows concentrations of Cs, Th, Pb, REE, Ta, Sc, Fe, Co, Cr, Ni in suspended sediments lower than those of the UC. Such an observation has already been reported in the black rivers of the Congo Basin and is probably due to the presence on the filters of abundant particulate organic matter that dilutes the other elements. Moreover, the Fe, Cr and Ni enrichments observed on Fig. 3 in the suspended sediments of the Rio Negro, Urucara and Trombetas are probably due to complexation by organic molecules.

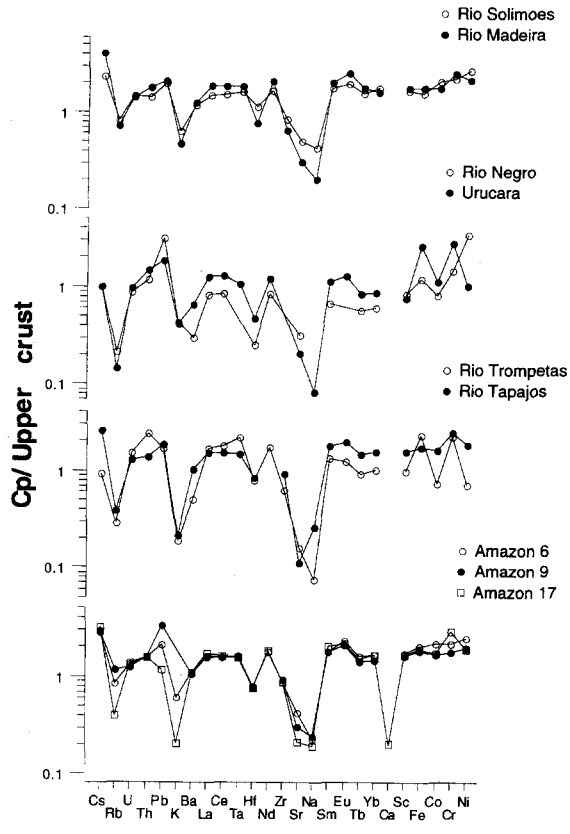

Fig. 3. Extended patterns of the suspended sediments of the Amazon rivers from this study. The upper continental crust is from Taylor and McLennan (1985). The *X*-axis order of elements corresponds to the enrichment from Ni to Cs of upper crustal concentrations with respect to the primitive mantle of the Earth (Hofmann, 1988). It is therefore an order of magmatic compatibility. This diagram allows to separate the most mobile elements during silicate weathering (U, Rb, Ba, K, Na, Sr, Ca) from the less mobile. The former are strongly depleted, whereas the latter are slightly enriched with respect to UC.

Finally, Zr and Hf are strongly depleted in the suspended sediments of the Amazon river system relative to UC, in agreement with previous observations in the suspended particles of the Congo Basin rivers (Dupré et al., 1996). Their depletion is most probably related to the absence of zircons (the main

Table 3
Major ion concentrations and Sr isotopic ratios measured in the dissolved load of the Amazon rivers (μmol/l)

Samples	pH	NO_3	SO_4	HCO_3	Cl	K	Na	Ca	Mg	SiO_2	Σ^+	Σ^-	NICB %	TDS mg/l	Denudation t/km^2/yr	$^{87}Sr/^{86}Sr$
Rio Negro	4.85	5	2		16	12	14	9	4	60	66	39	41	6	39	0.716223±70
Rio Negro tributary	4.43	4	2		16	7	9	9	1		18					0.727843±43
Solimoes swamp		4.5	17		47		73		34							
Solimoes	7.1		20	490	62	23	105	186	50	150	600	592	1	55	592	0.708776±25
Amazon 5 after Manaus	5.77	1	2		14		22	18	9		76					
Amazon 6 before Madeira	6.79		21	450	48	24	88	131	43	138	460	540	−17	48.3	540	0.709172±24
Rio Madeira	6.73		34	260	13	23	61	66	50	140	293	341	−16	33.2	341	0.720036±39
Amazon 8 after Madeira	6.78		25		33		78	118	46		406	428	−5		428	
Amazon 9	6.81		13	320	35		67		29			381			381	
Urucara	6.46		6	140	21	36	35	35	16	105	173	173	0	20.3	173	0.723584±29
Amazon 11	6.6		16	269	34		67		33			335			335	
Amazon 12 before Parintins	6.75		18	295	34		67		0			365			365	
Amazon 13	6.86		16		42	30	66		36							0.710728±34
Amazon 14	7.06		15	300	33	20	65		34			363			363	0.711120±18
Rio Trombetas	6.1		4	39	21	23	31	11	9	103	94	68	28	11.9	68	0.732295±55
Amazon 17 after Obidos	6.78		16	290	33		64	98	33		326	355	9		355	
Amazon 18 before Santarem	6.86		18	330	33		67		35			399			399	
Rio Tapajos	6.68		3	114	12	21	33	21	17	160	130	132	−2	9.1	132	0.733172±29
Amazon 20 after Santarem	6.89		15	280	32	22	65	89	33			342	−3		342	0.711478±20

$NICB = (\Sigma^+ - \Sigma^-)/\Sigma^+$.

Table 4
Trace element concentrations (ppb) measured in the dissolved phase of tributaries of the Amazon River

	Rio Negro			Negro tributary		Rio Solimoes			Rio Madeira			Urucara			Trombetas			Rio Tapajos	
	(1)	(2)	(3)	(1)	(2)	(1)	(2)	(3)	(1)	(2)	(3)	(1)	(2)	(3)	(1)	(2)	(3)	(1)	(2)
pH	4.85	4.85		4.43		7.10	7.10		6.73	6.73		6.46	6.46		6.10	6.10		6.68	
Li							1.0		1.2			0.4			0.4				
B							3.8		3.4			2.2			1.5				
Mg	102	95		38		1247	1142		1102	1185		394	419		192	218		469	
Al	114	116		117		184	171		3	7		53	48		39	51		15	
Mn	8	9		1		14	15			3		20	19		19	9		1	
Fe				29			351		18			266			87				
Co	0.12	0.14		0.04		0.14	0.16		0.02	0.02		0.10	0.08		0.13	0.12		0.02	
Ni	0.21			0.47		0.77	0.92		0.57	0.60		0.61	0.54		0.12	0.18		0.22	
Cu	0.40	0.31		0.41		1.72	1.54		0.86	1.58		0.47	0.59		0.27	0.38		0.23	
Zn	1.8	1.8		2.0		2.8	2.3		0.7	3.3		6.3	26.7		1.2	2.4		1.0	
Ga	0.005	0.010		0.003		0.040	0.039		0.003	0.005		0.005	0.008		0.006	0.013		0.003	
Rb	1.1	1.2		0.5		1.8	1.6		1.3	1.4		4.8	4.9		2.9	3.2		2.8	
Sr	3.6	3.7		0.7		46.0	45.7		19.2	19.6		13.4	13.3		6.7	6.8		9.9	
Ba	6.1	6.3		2.4		27.8	27.9		17.8	18.0		18.1	17.6		14.1	14.2		21.2	
La	0.15	0.14	0.151			0.19		0.166	0.05	0.05	0.054	0.18	0.18	0.178	0.28	0.26	0.266	0.22	
Ce			0.415		0.413			0.363			0.138			0.528			0.908		0.115
Pr			0.047		0.049			0.052			0.022			0.0511			0.08		0.0174
Nd	0.19	0.11	0.172	0.16	0.177	0.25		0.226	0.02	0.10	0.1	0.19	0.21	0.219	0.29	0.31	0.309	0.06	0.072
Sm			0.038		0.031			0.052			0.0311			0.0451			0.0596		0.0181
Eu			0.0088		0.0084			0.015			0.0083			0.0081			0.0105		0.0033
Gd			0.035		0.024			0.049			0.026			0.0364			0.0485		0.0114
Tb			0.004		0.0031			0.007			0.0048			0.005			0.0061		0.0015
Dy			0.023		0.019			0.044			0.024			0.032			0.044		0.0118
Ho			0.005		0.004			0.009			0.0053			0.0065			0.0093		0.002
Er			0.0147		0.0088			0.028			0.0134			0.0194			0.0283		0.0082
Tm			0.0024		0.0016			0.005			0.0025			0.0031			0.0041		0.0013
Yb			0.01		0.007			0.021			0.0092			0.0166			0.0264		0.0055
Lu	0.003		0.0016	0.003	0.0012	0.003		0.004	0.0003	0.002	0.0014	0.001	0.001	0.0022	0.003	0.004	0.0037	0.000	0.0009
Pb	0.170	0.145		0.348		0.147	0.151		0.005	0.089		0.089	0.165		0.052	0.084		0.061	
Th		0.055					0.010			0.014		0.079	0.091		0.121	0.128			
U	0.019	0.017		0.011		0.043	0.040		0.023	0.028		0.035	0.037		0.044	0.049		0.019	
K	487					927						1431					912	827	
Rb	1.1					1.6			1.3			4.8					3.1	2.6	
Sr	4.3					42.8			38.9			13.4					7.6	9.1	

(1) and (2) are replicates from the same sample.
(3) Run for REE analysis.

Hf- and Zr-bearing phase) in the suspended load and their presence in river sands (not analysed in this study).

(2) The Sm/Na ratio in suspended sediments normalized to the continental crust ratio [$(Sm/Na)_N$] gives the amplitude of the Na depletion in suspended sediments with respect to the mean continental crust. $(Sm/Na)_N$ can therefore be considered as an index of silicate weathering if we consider the continental crust as a good approximation of the eroded rocks over the drainage basin (see Section 7). $(Sm/Na)_N$ in the suspended load of the lowland rivers is close to 0.05, which is the typical value for the suspended sediments of the Congo Basin. By contrast, $(Sm/Na)_N$ in the Andean rivers (Solimoes, Madeira and the Amazon mainstream) are close to 0.1–0.2, indicating that weathering in the Andean zone is less intense than in the lowlands.

Table 5
Trace element concentrations (in ppb) measured in the dissolved phase of the Amazon River

	Amazon 5			Amazon 6		Amazon 20		
	(1)	(2)	(3)	(1)	(2)	(1)	(2)	(3)
pH	5.77			6.79		6.89	6.89	
Li	0.5	0.4		3.0		0.9		
B	1.4					1.6		
Mg	196	235		1037		755	806	
Al	122	139		21		9	10	
Mn	21	22		19		51	48	
Fe	30							
Co	0.21	0.22		0.07		0.18	0.16	
Ni	0.62	0.67		0.76		0.74	0.55	
Cu	0.68	0.86		1.43		1.46	1.53	
Zn	4.2	4.6		1.6		1.1	1.0	
Ga	0.013	0.009		0.015		0.017	0.011	
Rb	1.7	1.9		1.7		1.5	1.5	
Sr	7.3	7.8		37.7		25.8	25.5	
Ba	9.9	10.5		24.3		20.8	20.7	
La	0.36	0.40	0.366	0.14	0.145	0.10	0.10	0.106
Ce			0.933		0.218			0.218
Pr			0.095		0.032			0.031
Nd	0.39	0.46	0.387	0.17	0.136	0.11	0.13	0.136
Sm			0.085		0.035			0.0349
Eu			0.0158		0.008			0.0104
Gd			0.073		0.032			0.0356
Tb			0.0098		0.0047			0.0043
Dy			0.065		0.032			0.0333
Ho			0.0124		0.0059			0.0064
Er			0.035		0.0157			0.0181
Tm			0.0056		0.0031			0.0033
Yb			0.034		0.017			0.0159
Lu	0.005	0.005	0.0049	0.000	0.0025	0.002	0.003	0.0022
Pb	0.292	0.352		0.072		0.064	0.085	
Th	0.092	0.097		0.023				
U	0.046	0.052		0.045		0.052	0.054	
K				979		879		
Rb				1.6		1.8		
Sr				46.8		25.2		

(1) and (2) are replicates from the same sample.
(3) Run for REE analysis.

(3) The non-depleted elements have quite similar patterns in the Andean and lowland rivers, if we except Cs, Pb, Fe and Cr (enriched in the Urucara and Trombetas sediments) and Ni. Indeed, the Th/Sc normalized to its crustal value is constant and, in particular, is not correlated with the Nd model ages of the suspended sediments of each river. This absence of correlation contrasts with the correlation observed between the La/Yb ratio and Nd model age observed by Allègre et al. (1996). This shows that the variations in the REE patterns with Nd model age are not superimposed to variations of the whole pattern of elements.

4.2. Dissolved load

Major element concentrations and Sr isotopic compositions measured in the dissolved load are presented in Table 3. Trace element concentrations are given Table 4 for the tributaries and Table 5 for the Amazon mainstream.

4.2.1. Major element and Sr isotopes geochemistry—chemical denudation

The major element geochemistry of the Amazon Basin rivers has been extensively documented by Stallard (1980). Our data are in good agreement with these data measured in 1976–1977, and confirm the geochemical classification of the Amazon rivers proposed by Stallard (1980). Briefly, the Rio Negro, Negro Tributary, Urucara, Trombetas and Tapajos are very dilute rivers ($\Sigma^+ < 200$ μeq/l) with low pH (< 6.7), molar Ca/Na ratio < 1, and radiogenic $^{87}Sr/^{86}Sr$ isotopic ratios (0.716 for the Rio Negro, > 0.725 for the other rivers). The same chemical and isotopic features are found in the rivers of the Guayana Shield in the Orinoco Basin (Edmond et al., 1995). By contrast, the Rio Solimoes, Madeira and the Amazon mainstream exhibit higher dissolved ion concentrations ($\Sigma^+ > 300$ μeq/l), higher pH (> 6.7), a higher concentration of Ca than Na (Ca/Na > 1) and less radiogenic $^{87}Sr/^{86}Sr$ isotopic ratios. Note that the Sr isotopic ratios in the dissolved phase reported here are in good agreement with those measured by Palmer and Edmond (1992). For the entire Amazon Basin (at Santarem), a Sr isotopic ratio of $^{87}Sr/^{86}Sr$ of 0.71148 is measured, significantly lower than the value measured at Obidos by Palmer and Edmond, 0.7109. This discrepancy cannot be accounted for by the contribution of the Tapajos River and may be due to the seasonal variability. Finally, it is apparent from Table 3 that the sample Amazon 5 closely resembles the Rio Negro waters rather than a mixing between Solimoes and Rio Negro. This is chemical evidence for the difficulty of the waters of Rio Negro and Rio Solimoes to fully mix together.

The Rio Negro and Trombetas rivers are characterized by a significant charge imbalance, as indicated by the normalized inorganic charge balance (NICB) $[\Sigma^+ - \Sigma^-)/\Sigma^-]$ values of 40 and 30%, respectively. This imbalance is attributed to the abundance of organic anions, not analysed in Table 3. Important NICB values have also been reported in the organic-rich (coloured) waters of the Congo Basin (Probst et al., 1992; Dupré et al., 1996) and in the lowland rivers of the Orinoco Basin (Edmond et al., 1995).

In Table 3, the total chemical denudation rates are calculated using the total dissolved loads (TDS) and expressed in t km^{-2} yr^{-1}. The lowland rivers are characterized by very low denudation rates (6 t km^{-2} yr^{-1}), consistent with those determined in the Congo Basin and those measured in the Guayana

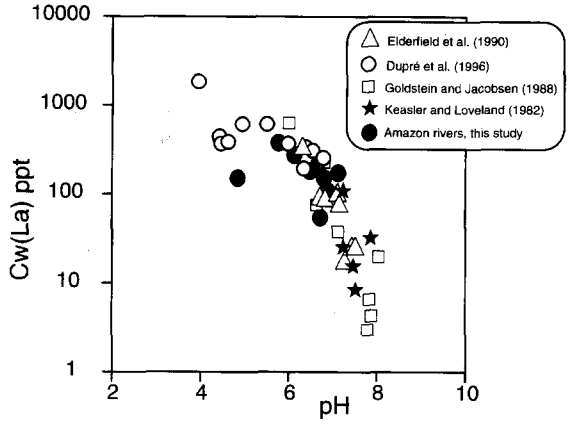

Fig. 4. Global relationship between dissolved absolute La concentration and pH for the rivers from this study and other world rivers. These data include the data from Elderfield et al. (1990) from North American and UK rivers, the data from Dupré et al. (1996) from the Congo Basin and the data from Keasler and Loveland (1982) from Northwest Pacific rivers. A clear linear relation is observed for pH > 6, while a larger degree of scatter appears for pH < 6.

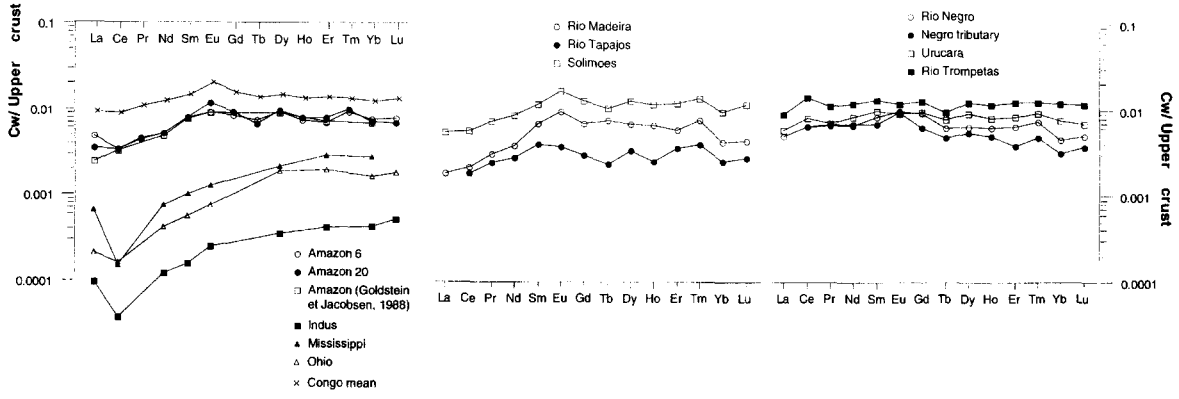

Fig. 5. REE patterns of the dissolved phase (0.2 μm filtered) for the rivers of this study. Data are normalized to UC. For comparison, this figure also includes the dissolved patterns reported in the Congo rivers (Dupré et al., 1996) and in some large rivers from Goldstein and Jacobsen (1988a). Note that the Amazon sample from Goldstein and Jacobsen (1988a) is in general agreement with the patterns reported here for the Amazon mainstream.

Shield by Edmond et al. (1995). These calculated rates of chemical denudation are higher in the Madeira and Solimoes basins: 23 t km^{-2} yr^{-1} and 67 t km^{-2} yr^{-1}, respectively. We will come back later to these denudation rates, which should not be considered as weathering rates.

4.2.2. Dissolved REE

The dissolved REE (Tables 4 and 5) concentrations in the Amazon rivers vary by more than an order of magnitude. The highest concentrations are observed in the Rio Solimoes, Rio Trombetas and Urucara. The less concentrated samples are from the Tapajos and Rio Madeira. The REE concentrations confirm the observation made earlier that the sample Amazon 5 more likely represents the Rio Negro and not the Amazon mainstream. The dependence of REE concentrations (e.g. La) on pH (Fig. 4) for the set of rivers studied here is compared to the dependence of REE dissolved concentrations on pH for a set of world rivers, including the rivers of the Congo Basin reported in Dupré et al. (1996). The rivers of this study have dissolved REE concentrations slightly lower than that of the Congo rivers, but among the

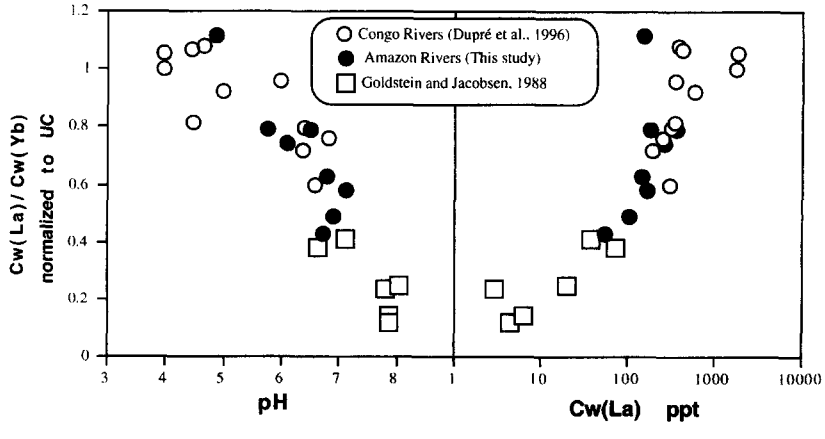

Fig. 6. Relation between the UC normalized La/Yb ratio and pH and dissolved La concentrations (ppt) for the rivers of this study, the rivers of the Congo Basin (Dupré et al., 1996) and the rivers studied by Goldstein and Jacobsen (1988a). This parameter is an index of the LREE depletion in the dissolved phase. Rivers of high pH are therefore characterized by low dissolved concentrations and highly HREE-depleted patterns, whereas rivers of low pH are characterized by high dissolved REE patterns and UC-like patterns.

highest at a global scale. They confirm the global decrease of REE dissolved concentrations (ranging on more than 4 orders of magnitude) with increasing pH, particularly for pH values greater than 6. For lower pH values, the data are more scattered. For example, the Rio Negro and Rio Solimoes have similar REE dissolved concentrations although their pH differs by 2 pH units. This observation indicates that, at least for pH < 6, pH is not the only parameter that controls river REE concentrations.

Dissolved REE patterns normalized to the UC are presented Fig. 5. Our data are consistent with the pattern reported for the Amazon river by Goldstein and Jacobsen (1988a). All patterns display a more or less pronounced upward convexity centred on the HREE, except the Rio Trombetas, which has a flat pattern. The Rio Solimoes, Madeira and Tapajos patterns show the strongest LREE depletions. The Rio Trombetas and Negro tributary are slightly depleted in the HREE. The pattern of the Amazon mainstream at Santarem confirms the major influence of the Solimoes and Madeira rivers, already observed using major elements. Other dissolved REE patterns from large rivers (Goldstein and Jacobsen, 1988b) are shown for comparison in Fig. 5 (Mississippi, Ohio, Amazon and Indus). We also reported the mean patterns of the Congo Basin rivers (Dupré et al., 1996). It appears that an increasing LREE depletion exists from the Congo rivers or the Trombetas and Urucara rivers [normalized La/Yb ratio: $(La/Yb)_N = 1$] to the Indus River [$(La/Yb)_N = 0.1$]. These variations are shown in Fig. 6, in which interesting correlations of $(La/Yb)_N$ with pH and absolute dissolved La concentration are observed for the rivers of this study, the rivers of the Congo Basin and the set of rivers from Goldstein and Jacobsen (1988a). These relations need to be more documented, but tend to indicate that river pH has a major control on the shape of the dissolved REE patterns and thus REE fractionation in the dissolved load.

4.2.3. Other elements

The other elements measured in the dissolved phase (Tables 4 and 5) are Li, B, Al, Mn, Fe, Co, Ni, Cu, Zn, Ga, Rb, Sr, Ba, Pb, Th and U. Previous dissolved concentration values have been reported for the Rio Negro and Solimoes by Konhauser et al. (1994). Our data are generally in good agreement with these data with a few exceptions. Zn concentrations reported here are 10 times lower than those

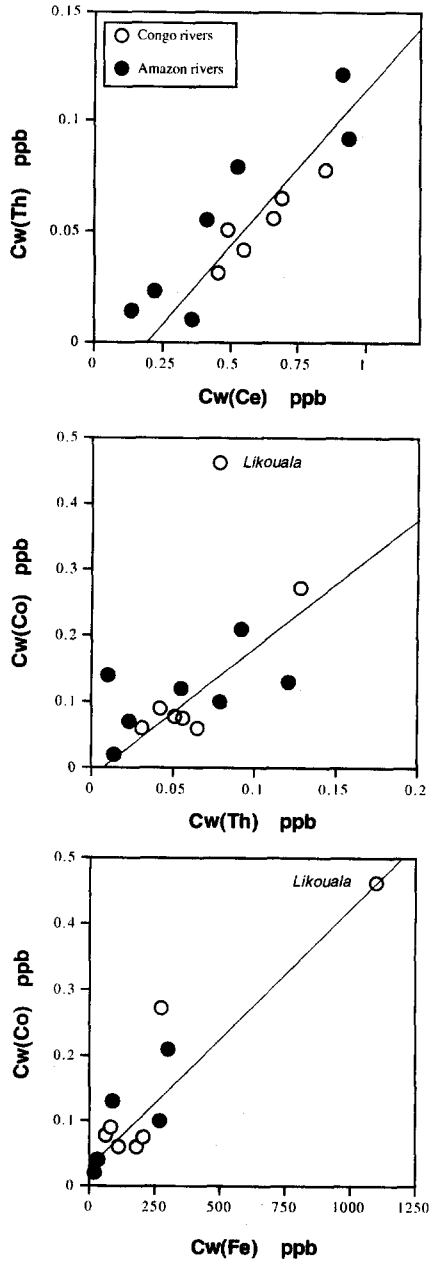

Fig. 7. Relationships between some trace elements in the dissolved phase of the Congo and Amazon rivers. It is interesting to observe the same relations for the Amazon and Congo basins. The Likouala River is a typical black river that shows the highest concentrations.

reported by Konhauser et al. (1994) for the Rio Negro above Manaus, and 3 times lower than that reported for the Rio Solimoes above Manaus. In the Rio Solimoes, our data for Mn, Fe and Pb are between 2 and 4 times lower than that reported by Konhauser et al. (1994).

In order to search for the relationships between these elements and the major and rare earth elements, the correlation coefficients between each pair of elements have been calculated. This leads to the following conclusions:

– Rb, Sr, Ba and U concentrations are strongly correlated with those of the major elements (Ca, Na, Mg, and alkalinity) and Σ^+. These correlations indicate that the abundance of these elements is controlled by the same processes that control the major ion chemistry (see Section 6). This is in agreement with the observation of Palmer and Edmond (1993) on U geochemistry in rivers.

– All other elements are decoupled from major ion chemistry. Among them, only Th and Co are well correlated with the REE. The correlations between Th and Ce, Co and Th, Co and Fe are shown in Fig. 7. The Congo data (Dupré et al., 1996) for the dissolved load have also been plotted for comparison. It is striking to note that rivers of both the Amazon and Congo basins follow the same trends.

Because Th has a very low solubility in natural waters (Langmuir and Herman, 1980; Dupré et al., 1996), the computation of the UC-normalized X/Th ratios allows a classification of the elements according to their mobility. For the set of rivers described here, Na, Ca, K, Ba, U, Sr, Rb, Li and B have Th-normalized ratios much higher than the corresponding crustal ratios, indicating that these elements are the most mobile. The elements Mn, Ni, Cu, Zn appear to have Th-normalized ratios about 10 times greater than the corresponding crustal ratios, indicating their low mobility. By contrast, Al, Fe, Ga, Pb and Co have Th-normalized ratios either close to the crustal value or lower. For example, the mean Al/Th-normalized ratio is close to 0.1, pointing out an observation already noted for the Congo rivers

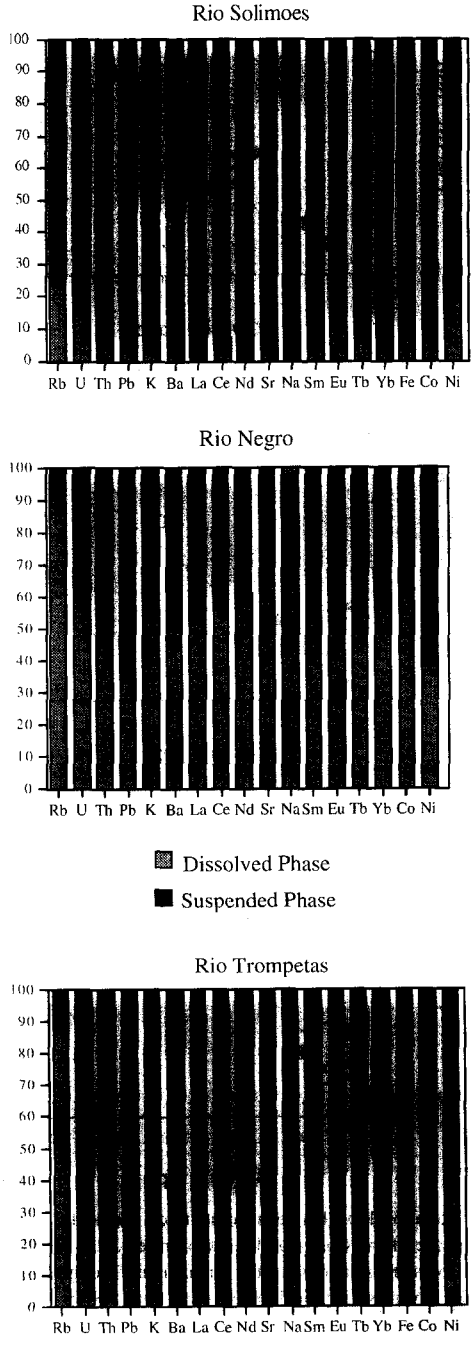

Fig. 8. Transport of the elements in three rivers from the Amazon Basin. For each element, for one litre of river water, the mass proportions of transport in the dissolved load and in the suspended phase are given. In order to calculate the suspended transport, the amount of suspended sediments (TSS) measured during the cruise (Table 1) is used. The main conclusion from this figure is the increase of suspended transport for the most insoluble elements from the Rio Solimoes to the Rio Negro.

(Dupré et al., 1996) that the dissolved phase is depleted in Al with respect to the continental crust.

4.3. Transport

An interesting aspect of the data presented in this paper is that the amount of each element transported by the dissolved and suspended loads can be compared. We calculated the mass of each element in one litre of river water as particles, by using the amount of suspended sediments measured during the sampling cruise (TSS, Tables 1 and 2). As we will see later, these concentrations are much lower than the values averaged over several years for the Solimoes, Madeira and Amazon mainstream. Results for the Rio Solimoes, Rio Negro and Rio Trombetas are shown in Fig. 8.

– Both suspended and dissolved phases contribute to the transport of Rb, Ba, K, Na, Sr, Ca and in a lesser extent U. This result is not surprising because these elements, as we already emphasized, are the most soluble elements and therefore the most mobile in the weathering processes.

– By contrast, the other elements, classically considered as non-mobile elements during weathering, are transported mainly in a suspended form in the Rio Solimoes, Rio Madeira, Rio Tapajos and in the Amazon mainstream. However, the proportion of these elements transported by the dissolved load is higher in the Rio Negro, Urucara and Rio Trombetas. For example, in the Rio Negro, the proportion of the HREE transported in dissolved form accounts for by 60% of the total flux. This feature is a result of the high dissolved concentrations measured in these rivers as well as of their low TSS concentrations. These results are similar to that observed in the organic-rich rivers of the Congo Basin, characterized by low amounts of suspended solids and high dissolved concentrations for the most insoluble elements.

5. Partition coefficients between dissolved and suspended loads

The data for the suspended and dissolved phases of each river presented above allow the calculation of 'partition coefficients' between soluble and suspended phases. This concept has been used in river chemistry for example by Whitfield and Turner (1979) and Martin and Whitfield (1983). We first focus on the REE and then compare the Cw/Cp patterns of the rivers of this study with those of Dupré et al. (1996) for the Congo rivers and those of Goldstein and Jacobsen (1988b) for other large river systems.

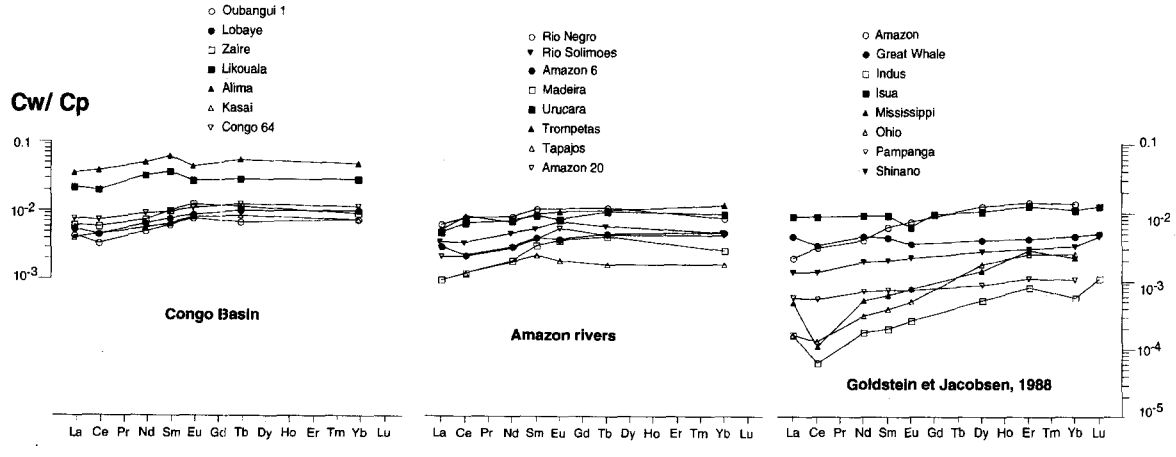

Fig. 9. Dissolved REE concentrations normalized to suspended concentrations for each river of this study, for the Congo river (Dupré et al., 1996) and for some other large rivers (Goldstein and Jacobsen, 1988b). Cw is expressed in ppb, Cp in ppm. A large range of REE fractionation is observed among these rivers with an increased LREE depletion from the Isua or Likouala River to the Indus. In terms of LREE depletion, Amazonian rivers have an intermediate feature between the rivers of the Congo and the rivers having lower concentrations.

5.1. Rare earth elements

The dissolved REE concentrations are normalized to the suspended ones in Fig. 9 (Cw/Cp diagram where Cw and Cp are the concentrations in the dissolved and suspended phase respectively). None of the Cw/Cp patterns is flat, pointing out the existence of slight REE fractionations during weathering and transport by rivers. All patterns are more or less LREE-depleted, particularly the Amazon mainstream and Madeira River. The dissolved La/Yb ratio normalized to that of suspended sediments ($K_{La/Yb} = La/Yb_{solution}/La/Yb_{solid}$) range from 0.4 (Amazon mainstream, Rio Madeira) to 0.8 (Rio Negro). This feature is in agreement with the observations of Dupré et al. (1996) for the Congo rivers (mean $K_{La/Yb} = 0.7$) and with a number of rivers studied by Goldstein and Jacobsen (1988a). Among these latter rivers, only the Great Whale is characterized by $K_{La/Yb} = 1$. The Amazon River pattern reported by Goldstein and Jacobsen is more LREE-depleted ($K_{La/Yb} = 0.15$) than any pattern reported in this study. At a global scale, a trend of increasing depletion of dissolved HREE relative to suspended sediments (of decreasing $K_{La/Yb}$ value) with increasing pH (or decreasing absolute REE abundance) is therefore apparent in rivers. This trend is similar to the one reported in Fig. 6, but it has a larger degree of scatter. Such relationships need to be confirmed by more data on world rivers, but strongly suggest that pH controls the fractionation of REE in rivers. At least two mechanisms can be proposed to explain such a control: adsorption processes, whose importance increases with pH (Schindler and Stumm, 1987), and the existence of organo-mineral colloids which exist in a dispersed form at low pH and tend to agglomerate and coagulate with increasing pH. Ultrafiltration experiments carried out by Sholkovitz (1992, Sholkovitz, 1995) demonstrated the evidence of such a phase in North American rivers, and showed that this phase has a shale-like REE pattern. By contrast, the true dissolved patterns for REE displays an important LREE depletion ($K_{La/Yb}$ = 0.01 to 0.05), similar to that observed in the rivers of high pH values (Indus River).

A crude approach is therefore to consider that the dissolved REE concentrations in the Amazon rivers of this study consist of a mixing between a true dissolved pool ($K_{La/Yb} = 0.05$) and a colloidal pool ($K_{La/Yb} = 1$). This type of calculation has been applied to the Congo rivers (Dupré et al., 1996) and allows the proportion of colloidal Yb (with respect to the total dissolved Yb) for the Amazon rivers to be calculated. Proportions ranging from 30 to 40% in the Rio Madeira and Amazon mainstream (the most HREE-depleted rivers) to 80% in the Rio Negro are then necessary to account for the Cw/Cp patterns reported in this study. In the future, we hope to carry out ultrafiltration experiments, using different pore size filters, to confirm these proportions and to understand the way REE are transported in big rivers. Finally, if such large proportions of REE are transported in the so-called colloidal phase, then the concept of a partition coefficient appears inappropriate, as it depends on the filtration pore size.

5.2. Other elements

In Fig. 10, the normalisation of dissolved concentrations to suspended ones has been extended to the other elements. This figure only shows the average of the Amazon river systems. This diagram is similar to that reported by Dupré et al. (1996) for the Congo river system. This diagram points out the enrichment of the most mobile elements (Ca, Na, Sr, Ba, K, U, Rb) in the dissolved phase with respect to the sus-

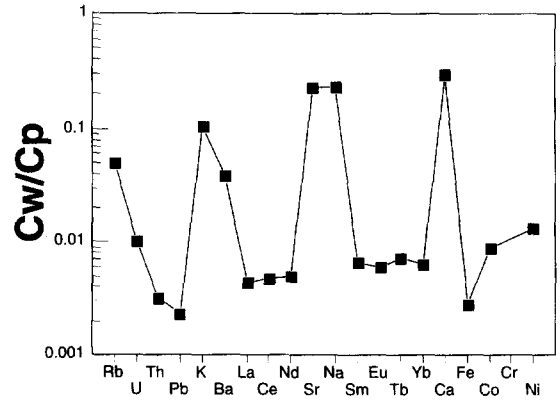

Fig. 10. Averaged dissolved concentrations normalized to average suspended concentrations for the whole set of rivers from this study. This diagram points out the enrichment of the most soluble elements. The other elements display flat or slightly enriched patterns. A Fe depletion is observed, consistent with previous observations in the Congo Basin.

pended phase. The abundances of these elements are controlled by atmospheric and rock dissolution inputs as will be shown in Section 6. The other elements show a gradual increase of Cw/Cp from Th and Pb to Ni. This enrichment can not be fully explained using the data reported here and further studies would require ultrafiltration experiments. Nevertheless, the above conclusions inferred from the REE patterns can be extended to the other elements. Thorium, in particular, has a very limited solubility and its presence in the dissolved load at concentrations close to 10–100 ppb in the rivers of this study strongly supports the existence of a colloidal phase. The enrichment of Ni and Cr in the dissolved phase with respect to Th is therefore either due to their enrichment in colloids, or to the contribution of a true dissolved pool for these elements (as for HREE). This dissolved pool may include Ni associated with dissolved organic material.

Iron appears to be depleted in the dissolved phase with respect to the suspended phase (Fig. 10). The same feature has been reported in the Congo Basin by Dupré et al. (1996) and points out an Fe depletion of the colloidal phase.

Again, the concept of 'partition coefficients' is inappropriate to describe the behaviour of the above elements in rivers such as the Congo and Amazon.

6. Source control on the dissolved load. chemical weathering rates of silicates

In this section, we discuss the relationships observed in the Amazon rivers between the most soluble elements in terms of atmospheric inputs and rock sources. Our approach is close to a previous one, already applied in Négrel et al. (1993) to the Congo Basin. The key point of this approach is the search for mixing relationships in river waters in various diagrams using elemental ratios and Sr isotopes.

The pioneering work of Stallard (1980) and Stallard and Edmond (1983, 1987) has highlighted the importance of atmospheric inputs (cyclic salts) and lithology to the dissolved load of rivers in the Amazon Basin. This conclusion is also reached by Palmer and Edmond (1992) in their study of Sr isotope systematics of Amazon waters. We propose in the following, an inversion method that combines the information provided by major ion geochemistry and that provided by Sr isotopic composition. This technique will allow us to quantify the mixing of atmospheric and rock-derived materials in the rivers of the Amazon Basin.

6.1. Atmospheric inputs to river chemistry

As previously shown by numerous authors (Stallard, 1980; Meybeck, 1983), Cl, whose concentration in rocks is very low, is the most useful reference to evaluate atmospheric inputs to rivers. Difficulties arise when evaporites are present in the river drainage, which is evident for the Andean rivers (Stallard, 1980). As shown by Stallard and Edmond (1987) in South America, Meybeck (1986) in Western Europe and Négrel et al. (1993) in Central Africa, Cl, originating from the dissolution of atmospheric seasalt particles by rainwaters, shows concentrations decreasing with increasing distance from the coast. In the Amazon River Basin, as determined by Stallard and Edmond (1983), the average Cl concentration in rainfall is 10 μmol l^{-1}, 1500 km inland. In order to determine the atmospheric Cl inputs to rivers of the Amazon Basin, two complementary ways can be used. The Cl concentration of rain at a given point in the basin can be multiplied by the evapotranspiration factor to evaluate the concentration in the river. In the Amazon Basin, this factor is close to 2.2 (Salati and Marques, 1984). The Cl content of rainwaters in the Amazon River Basin has been measured by numerous authors (Stallard, 1980; Furch, 1984; Galloway et al., 1982; Andrae et al., 1990; Forti and Moreira-Nordemann, 1991; Lesack and Melack, 1991), and based on 260 rain samples, the mean values for each element are listed in Table 6. The mean Cl concentration is 8.3 μmol l^{-1} and leads then to a mean atmospheric input in rivers of 18 μmol l^{-1}.

The other method to determine the atmospheric input of Cl in rivers is simply to consider rivers that do not drain saline formations. This requires knowledge of the drainage basin lithology, which is not trivial. Fortunately, such rivers exist in the Amazon Basin, as shown by Stallard (1980). The Coari, Tefe, Rio Negro and Branco, Xingu, Trombetas and numerous small rivers in the Andes exhibit Cl concentrations ranging from 20 μmol l^{-1} to 6 μmol l^{-1}

from west to east, consistent with the concentrations estimated from rainwater data.

In this study, when Cl river concentration does not exceed 20 μmol l^{-1} (Cl_{crit}), Cl will be considered as totally derived from marine aerosols. For Cl river concentrations greater than 20 μmol l^{-1}, evaporite rock dissolution is invoked to supply Cl to the river.

The rainwater contribution can be constrained using the mean values calculated in Table 6 for the rainwaters of the Amazon Basin. The typical ratios are $Cl/Na = 1.24 \pm 0.1$, $Ca/Na = 0.25 \pm 0.03$, $Mg/Na = 0.13 \pm 0.01$. Strontium concentrations in Amazon Basin rainwaters have been reported by Furch (1984) and lead to Sr/Na molar ratios close to 0.003 ± 0.001. Compared to the corresponding marine ratios ($Cl/Na = 1.16$, $Ca/Na = 0.023$, $Mg/Na = 0.11$, $Sr/Na = 0.00019$), the Amazon rainwaters appear to be enriched in Ca, Mg and Sr. This observation confirms the conclusions of Négrel et al. (1993) in the Congo Basin and reflects the contribution of carbonate-rich aerosols to rainwaters.

One important concern of atmospheric correction to the dissolved load of rivers is to know whether the dissolved load of rivers must be corrected for atmospheric inputs using local rainwater composition (by the use of Cl-normalized rainwater ion ratios) or from its oceanic part (by the use of Cl-normalized seawater ratios). Applying a marine correction to the dissolved river load means that the surpluses of Ca, Mg, K, Sr and other trace elements in rainwater originate from the drainage basin itself and that these elements are part of the continental weathering flux. For these reasons, a marine correction is attempted in this paper. The present day marine Na-normalized and Sr isotopic ratios (0.70917) have been used to correct the atmospheric contribution to river dissolved load.

6.2. Rock weathering inputs

In a global approach (Garrels and MacKenzie, 1971) the three main lithologies undergoing chemical weathering are silicates, limestones and evaporites. The waters draining each of these rock types are characterized by their own chemical and Sr isotopic signature. This signature depends on both the chemical composition of the bedrock and on the rate at which it is eroded. Carbonate rocks and evaporites are weathered 12 times and 40 to 80 times, respectively, more rapidly than granites or gneisses, according to the estimations of Meybeck (1987). As a consequence, evaporites have a major influence on river chemistry even if their outcrops are rather rare and concentrated in mountains.

The Sr isotopic ratio, Ca/Na, HCO_3/Na and Mg/Na ratios are particularly well suited to distinguish between carbonate, silicate or rain and have the very important property of being independent of water fluxes and then dilution of evaporation effects. Following the technique initiated in Négrel et al. (1993), in Fig. 11 we present the relationships between Sr isotopic composition and Ca/Sr, and between Ca/Na, HCO_3/Na and Mg/Na ion ratios for

Table 6
Chemical composition of rainwaters in the Amazon Basin (μmol/l)

Origin of data	*n*	Stage	Cl	Ca	Na	Mg	Sr
Lacaux et al. (1992)	35	total	4.7	2	4	–	–
Lesack and Melack (1991)	89	wet	4	0.95	1.9	0.65	–
Lesack and Melack (1991)	34	dry	8.2	1.45	5.1	1.05	–
Stallard and Edmond (1980)	32	total	13.7	1.1	12.4	1.2	–
Galloway et al. (1982)	14	total	2.5	0.15	1.8	0.25	–
Forti and Moreira-Nordemann (1991)	16	wet	15.3	3.33	29.5	1.61	–
Forti and Moreira-Nordemann (1991)	10	dry	36.5	6.46	20.4	2.22	–
Forti and Moreira-Nordemann (1991)	18	wet	7.73	2.4	3.13	0.31	–
Forti and Moreira-Nordemann (1991)	11	dry	11.8	3.07	9.57	0.76	–
Furch (1984)	25	total	–	1.8	5.2	0.88	0.008
Weighted average excluding Furch (1984)	259		8.31	1.68	6.73	0.88	–

the rivers of the Amazon Basin studied by Stallard (1980) for major ion chemistry, and Palmer and Edmond (1992) for Sr isotopic composition (43 river samples) together with our data (11 samples). In such diagrams (Fig. 11b,c), mixing between two endmembers is represented by a straight line as the same element (Na) is used as a normalization. The most probable range of rock weathering endmembers for silicates, carbonates and evaporites has been estimated combining the mixing trends of Fig. 11 and literature data based on simple or well constrained lithologies. These data include the Andean streams from Stallard (1980) and Stallard and Edmond (1983), the data from rivers draining the Guayana Shied (silicates only) from Edmond et al. (1995), the small rivers from remote areas in France reported by Meybeck (1986), and the data on small rivers draining carbonates and silicates in the Congo Basin (Négrel et al., 1993). When corrected for atmospheric inputs, the data from monolithological streams allow us to estimate the variability of the Na-normalized ratios and Sr isotopic ratios for each type of lithology. Salt springs and streams with Cl concentrations greater than 1000 μmol l^{-1} are reported by Stallard (1980) in the Ucallayi and Maranon Andean drainages. Both their ion content and Sr isotopic ratios (Palmer and Edmond) allow the evaporite endmember to be estimated (Fig. 11). This endmember is characterized by $Ca/Na = 0.17 \pm 0.09$, $Mg/Na = 0.02 \pm 0.01$, $Sr/Na = 3 \pm 2 \times 10^{-3}$, $HCO_3/Na = 0.3 \pm 0.3$ and $^{87}Sr/^{86}Sr = 0.7081 \pm 0.0005$. In the same way, the carbonate endmember can be evaluated as having the following typical ratios: $Ca/Na = 45 \pm 25$, $Mg/Na = 15 \pm 10$, $Sr/Na = 40 \pm 20 \times 10^{-3}$, $HCO_3/Na = 90 \pm 40$ and $^{87}Sr/^{86}Sr = 0.7075 \pm 0.0005$. The shield silicate endmember is characterized by $Ca/Na = 0.35 \pm 0.25$, $Mg/Na = 0.24 \pm 0.16$, $Sr/Na = 3 \pm 1 \times 10^{-3}$, $HCO_3/Na = 1 \pm 1$ and $^{87}Sr/^{86}Sr = 0.730 \pm 0.01$. The silicate-draining water endmember for the

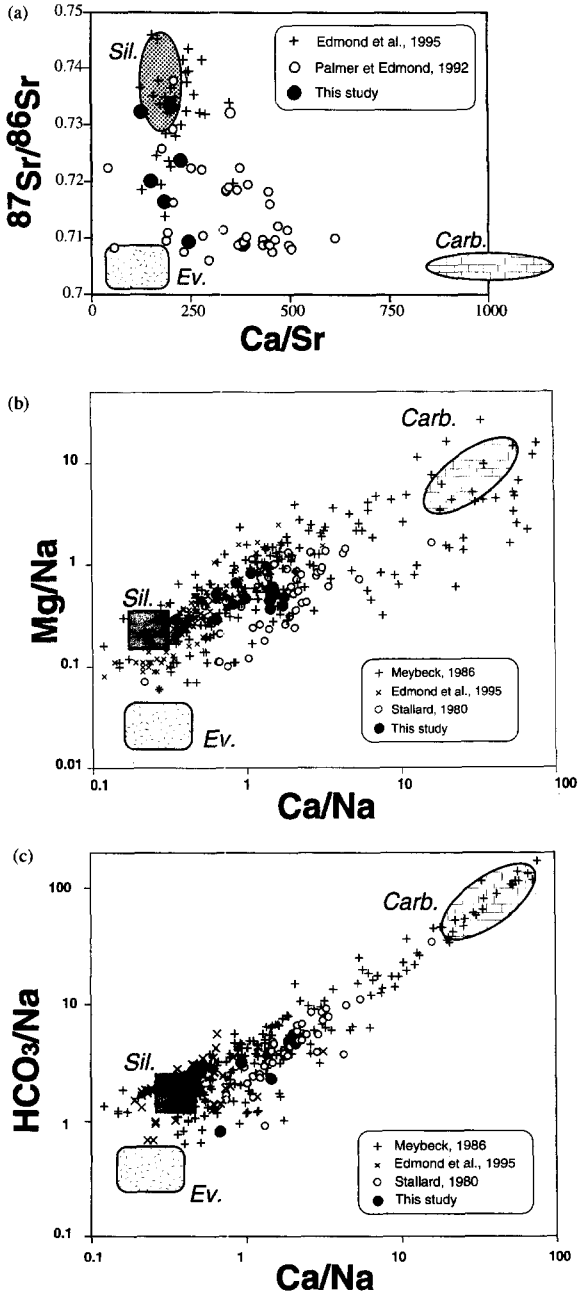

Fig. 11. Mixing diagrams of the dissolved load comparing the data from the present study to the data from Stallard (1980) and Palmer and Edmond (1992) in the Amazon River Basin. Mixing endmembers are constrained using the data from Meybeck (1986) on small western Europe catchments, and the data from Edmond et al. (1995) in rivers draining the Guayana Shield (silicates). These two sets of data are corrected from atmospheric inputs using Cl as a reference. (a) Sr isotopic ratio versus molar Ca/Sr The silicate endmember represents the shield silicate endmembers. The silicates from the Andes (young volcanics and plutonics) are expected to deliver less radiogenic Sr to the rivers, close to 0.706 ± 3 (see text). (b, c) Mg/Na vs. Ca/Na and HCO_3 /Na vs. Ca/Na molar ratios.

Solimoes and Amazon mainstream is expected to be different, because both the source rocks (Andean calc-alkaline volcanics and plutonics) and weathering conditions of these drainages are different. The chemical or Sr isotopic studies of waters flowing over recent volcanics (Meybeck, 1986; Goldstein and Jacobsen, 1987; Gislason et al., 1996; Louvat and Allègre, 1997) show that their Sr isotopic composition is very close to that of the bedrock and that their Na-normalized ratios, independently of climate and relief, are slightly elevated compared to those of the shields. For example, typical Ca/Na ratios for the waters draining volcanics range between 0.3 and 0.8 (Louvat and Allègre, 1997). Based on these considerations, and the fact that the Andes constitute only a small part of the Solimoes and Amazon drainages, the endmember parameters for the Solimoes and Amazon 6 are taken as $Ca/Na = 0.5 \pm 0.3$, $Mg/Na = 0.5 \pm 0.2$, $Sr/Na = 5 \pm 2 \times 10^{-3}$, $HCO_3/Na = 2 \pm 1$ and $^{87}Sr/^{86}Sr = 0.706 \pm 0.003$.

Finally, slightly different silicate endmember ratios for the Rio Negro drainage have been chosen from those of the shield rivers. At least two arguments can be invoked for that. On the one hand, the Rio Negro drains mostly intensely weathered areas composed of Tertiary sediments depleted in cations (more depleted in Na, than Ca, due to their respective mobilities) and on the other hand dissolved organic matter is abundant within the drainage and probably increases mineral weathering. Similar organic-driven weathering regimes have been described in Africa by Viers et al. (1997). The results of this study show that the Na-normalized ratios of solutes are elevated compared to less-organic dominated environments. According to these considerations, the Na-normalized ratios are chosen as $Ca/Na = 1 \pm 0.5$, $Mg/Na = 0.6 \pm 0.3$, $Sr/Na = 5 \pm 2 \times 10^{-3}$, $HCO_3/Na = 3 \pm 1$.

6.3. Model equation and resolution

Mass budget equations can be written to calculate the amount of each element originating from the different reservoirs: rainwater, silicate weathering, limestone weathering and evaporite weathering. We simply state that the amount (per litre of water) of a solute in riverwater is the sum of the contribution for each reservoir. If the subscripts riv, rw, sil, carb, and ev denote the river, rainwater, silicate, carbonates and evaporites, respectively, then $X_{riv} = X_{rw} + X_{ev} + X_{sil} + X_{carb}$, for any element X = Na, Cl, Ca, Mg, HCO_3 and Sr.

If the river Cl concentration is greater than Cl_{crit} then $Cl_{riv} = Cl_{rw} + Cl_{ev}$, if the river Cl concentration is $< Cl_{crit}$ then $Cl_{riv} = Cl_{rw}$.

The last equation describes the mass budget of Sr isotopic ratios:

$$\left(\frac{^{87}Sr}{^{86}Sr}\right)_{riv} Sr_{riv} = \left(\frac{^{87}Sr}{^{86}Sr}\right)_{rw} Sr_{rw} + \left(\frac{^{87}Sr}{^{86}Sr}\right)_{ev} Sr_{ev} + \left(\frac{^{87}Sr}{^{86}Sr}\right)_{sil} Sr_{sil} + \left(\frac{^{87}Sr}{^{86}Sr}\right)_{carb} Sr_{carb}$$

In the following, this equation is solved by an inversion procedure using elemental ratios instead of absolute concentrations, as presented in Négrel et al., 1993. This technique, now widely used in geochemistry (Allègre et al., 1983; Allègre and Lewin, 1989), is particularly well suited for such a resolution because, as we saw earlier, the endmembers are not completely determined. In such an approach, there are no data and unknowns. All variables are parameters for which we have more or less information. The only reasonably well known parameters are the river parameters. By contrast, the ion ratios and isotopic ratios of the endmembers estimated in the previous section are poorly known and thus the size of the error reflecting the possible range of variation will be large. The aim of the inversion procedure is to make all budget equations compatible and to improve our knowledge of the poorly known parameters. The so calculated parameters and their errors are named a-posteriori parameters and errors.

6.4. Results

For each river, the inversion procedure makes it possible to find a solution to the different mixing equations. The proportions of Na, Ca, HCO_3, Mg and Sr originating from the different reservoirs for the rivers of this study are given in Table 7. Several observations arise from this table.

– The dissolution of evaporites plays an important role in the Solimoes River and in the Amazon mainstream. The Madeira River does not appear to

be influenced by evaporite dissolution. In the Amazon River at Santarem, it is found that 12 ± 8% of the Sr originates from the Andean saline formations. In the shield, the Sr derived from saline rocks is not significant.

– The dissolution of carbonates influences the dissolved load of each river reported here. The rivers of the Subandean zone and Andean Cordillera have the greatest proportions of Ca, Mg, Sr derived from carbonates, in agreement with the lithology. In the shield areas, the major part of Ca appears to derive from carbonate weathering.

– Silicate weathering contributes to the dissolved Sr concentration from 50% in the Solimoes to 85–87% in the Tapajos and Trombetas rivers. The isotopic composition of the silicate endmember can be constrained by the inversion scheme. Isotopic compositions greater than 0.720–0.735, consistent with the values calculated in the Congo Basin are obtained for the shield rivers and Madeira River. By contrast, lower $^{87}Sr/^{86}Sr$ isotopic ratios are calculated for the Solimoes River and for the Amazon (ca. 0.711). These isotopic contrasts highlight the influence of the recent eruptive activity in the Amazon Basin. This result shows the contribution to the dissolved load of Sr derived from the Andean erup-

Table 7
Proportions of each element derived from the atmosphere and from silicate, carbonate and evaporite weathering deduced from the mixing model (Section 6)

River		Na	Ca	HCO_3	Mg	Sr
Negro	atm	54 ± 9	2 ± 1		22 ± 5	3 ± 1
	carb	0	24 ± 20		15 ± 10	4 ± 4
	sil	46 ± 9	75 ± 30		63 ± 27	93 ± 10
Solimoes	atm	16 ± 3	0	0	4 ± 1	0
	ev	38 ± 6	3 ± 2	3 ± 2	2 ± 1	20 ± 13
	carb	3 ± 1	86 ± 5	72 ± 8	54 ± 19	30 ± 6
	sil	25 ± 8	11 ± 4	25 ± 8	41 ± 19	49 ± 14
Amazon 6	atm	18 ± 3	0	0	4 ± 1	1 ± 1
	ev	29 ± 5	3 ± 2	2 ± 2	1 ± 1	16 ± 6
	carb	3 ± 1	85 ± 6	61 ± 8	49 ± 20	22 ± 4
	sil	50 ± 6	12 ± 6	36 ± 8	46 ± 20	61 ± 8
Rio Madeira	atm	17 ± 3	0	0	3 ± 1	1 ± 1
	carb	3 ± 1	84 ± 10	49 ± 8	69 ± 15	24 ± 6
	sil	80 ± 4	16 ± 10	52 ± 8	28 ± 15	75 ± 6
Urucara	atm	38 ± 6	1 ± 1	0	10 ± 2	2 ± 0,5
	carb	2 ± 1	88 ± 7	56 ± 8	62 ± 18	29 ± 5
	sil	55 ± 6	11 ± 7	44 ± 8	29 ± 18	66 ± 7
Rio Trombetas	atm	50 ± 6	3 ± 1	0	21 ± 5	4 ± 1
	carb	1 ± 1	69 ± 25	41 ± 17	35 ± 21	9 ± 4
	sil	49 ± 6	28 ± 25	59 ± 17	45 ± 22	87 ± 5
Rio Tapajos	atm	30 ± 4	0	0	7 ± 1	1 ± 1
	carb	1 ± 1	71 ± 22	72 ± 24	51 ± 19	14 ± 5
	sil	69 ± 5	28 ± 22	27 ± 20	42 ± 15	85 ± 5
Amazon 20	atm	27 ± 4	0	0	7 ± 2	1 ± 1
	ev	19 ± 4	2 ± 1	1 ± 1	1 ± 1	12 ± 8
	carb	2 ± 1	84 ± 4	79 ± 9	61 ± 22	25 ± 5
	sil	51 ± 6	14 ± 4	20 ± 9	31 ± 22	63 ± 10

tive rocks having Sr isotopic ratios close to 0.705 (Soler and Rotach-Toulhoat, 1990). As shown by Goldstein and Jacobsen (1987, 1988a) or Louvat and Allègre (1997), the soluble (and particulate) isotopic composition of Sr draining volcanic rocks is similar to that of the bedrock.

– For the Rio Negro, Cl and Na concentrations are very low and very similar. As a consequence, and once corrected from the marine inputs, Na concentration is close to zero, while Ca is not affected. As a result the Ca/Na ratio is high, and can be interpreted as indicating the importance of carbonate weathering, which is not consistent with what we know about the Negro drainage lithology. If a rain correction is applied (using the concentrations in rainwaters from Table 6), the corrected Ca/Na ratio decreases (0.97) significantly because of the contribution of Ca-bearing aerosols to Amazon rainwaters, but is still higher than the estimated Ca/Na ratio of waters draining silicates. The proportions given in Table 7 have therefore major uncertainties, due to the extreme sensitivity of the Rio Negro waters to the correction of atmospheric inputs. Clearly for organic-dominated and very dilute rivers such as the Rio Negro (or Likouala and Sangha rivers in the Congo Basin), additional studies are necessary. In particular, one well-posed challenge is to better estimate the range of variation of the silicate endmember in such highly weathered and organic-rich environments.

Finally, the influence of the seasonal variability of dissolved concentrations has been tested on the above-calculated proportions. Devol et al. (1995) have reported the results on dissolved depth-integrated concentrations of a multi-year time series (1983–1993) study of the Solimoes near Manaus. This data base allowed us to show that the Na-normalized ratios in the Solimoes differs by less than 10% from the ratios calculated using our data, indicating that the seasonal variability does not modify drastically the above calculations.

6.5. Weathering rates and inorganic CO_2 consumption

The proportions calculated above allow the total dissolved ions (TDS) derived from each lithology to be calculated. The weathering rates are denoted TDS_{sil} (for silicates), TDS_{carb} (for carbonates) and TDS_{ev} (for evaporites) and are expressed in mg/l, in t/y or in t km^{-2} yr^{-1}. The silicate and carbonate weathering rates are shown in Table 8 and Fig. 12. TDS_{sil} ranges from 1 to $5 \cdot 10^6$ t/yr (6 t km^{-2} yr^{-1}) in the lowland rivers to $43 \cdot 10^6$ t/yr (20 t km^{-2} yr^{-1}) in the Solimoes. The value corresponding to the Amazon at Santarem is $70 \cdot 10^6$ t/yr (15 t km^{-2} yr^{-1}). These rates for the silicate part of the drainage basin are consistent with those determined by Edmond et al. (1995) in the rivers of the Guayana Shield after correction from atmospheric inputs. They are also in agreement with those calculated in the rivers of the Congo Basin (Gaillardet et al., 1995). The TDS_{carb} fluxes are systematically lower than the TDS_{sil} except for the Solimoes River where $TDS_{carb} = 1.4 \times TDS_{sil}$. Finally TDS_{ev} are significant only for the Solimoes and Amazon mainstream but are at least one order of magnitude lower than the flux due to silicates.

The inorganic consumption of CO_2 by rock weathering can be calculated using the proportions of HCO_3^- derived from silicates and carbonates calculated above. Following the reaction

$$(Ca,Mg)CO_3 + CO_2 + H_2O \rightarrow (Ca^{2+},Mg^{2+}) + 2HCO_3^-$$

the dissolution of carbonates produces two moles of HCO_3^- for one mole of $Ca^{2+} + Mg^{2+}$, but only one is derived from the atmosphere. By contrast all the alkalinity derived from silicates originates from the atmosphere. The calculated fluxes are given Table 8 and Fig. 12. The total flux of CO_2 derived from rock weathering ranges from 6 to $30 \cdot 10^9$ mol/yr in the lowland rivers to about $1000 \cdot 10^9$ mol/yr for the Solimoes. The flux consumed by silicate weathering only ranges from $4.5 \cdot 10^9$ mol/yr for the Trombetas to $670 \cdot 10^9$ mol/yr for the Amazon 6. As the precipitation of calcite in the oceans balances the riverine input of HCO_3 (and Ca) derived from carbonates, the flux of CO_2 removed from the atmosphere by silicate weathering must be considered as the net CO_2 consumption flux by the weathering of continents (Berner, 1994). According to our results, for the entire Amazon Basin, the weathering of silicates consumes about $320 \cdot 10^9$ mol/yr. This flux is dominated by the inputs of the Solimoes and

Table 8
Total dissolved solids and CO_2 consumption rates derived from chemical weathering of all lithologies (total) and from the chemical weathering of silicates (sil) or carbonates (carb)

River	Water discharge (m^3/s)	Drainage area (10^3 km^2)	TDS_{total} (mg/l)	CO_2 total (10^9mol/yr)	TDS_{sil} (mg/l)	TDS_{sil} (10^6t/yr)	CO_{2sil} (10^9mol/yr)	TDS_{sil} (t/km^2/yr)	S	TDS_{carb} (mg/l)	TDS_{carb} (10^6t/yr)	CO_{2carb} (10^9mol/yr)
Negro	28400	696.81	4.6	0	4.3	4	0	0.6	0	0.3	0.3	0
Rio Solimoes	103000	2147.74	32.7	996	13.2	43	400	20	0.11	18.3	59	600
Amazon 6	131300	2854.3	27	1267	12.3	51	670	18	0.16	13.8	57	600
Rio Madeira	31200	1420	19.7	194	12.8	13	133	8.9	0.12	6.9	7	61
Urucara	3000	150	12.6	9.6	8.7	1	5.6	5.5	0.07	3.9	0.4	3.7
Trombetas	6200	250	8.7	6.1	7.8	1.5	4.5	6.1	0.04	0.9	0.2	1.6
Tapajos	13500	490	14.8	31	11.5	4.9	13.2	10	0.03	3.4	1.4	18
Amazon 20	182200	4618.75	22.3	965	12.1	70	320	15	0.06	10.2	59	644

The index S corresponds to the ratio of the CO_2 consumption flux divided by the silicate weathering flux. This parameter does not depend upon the silicate area.

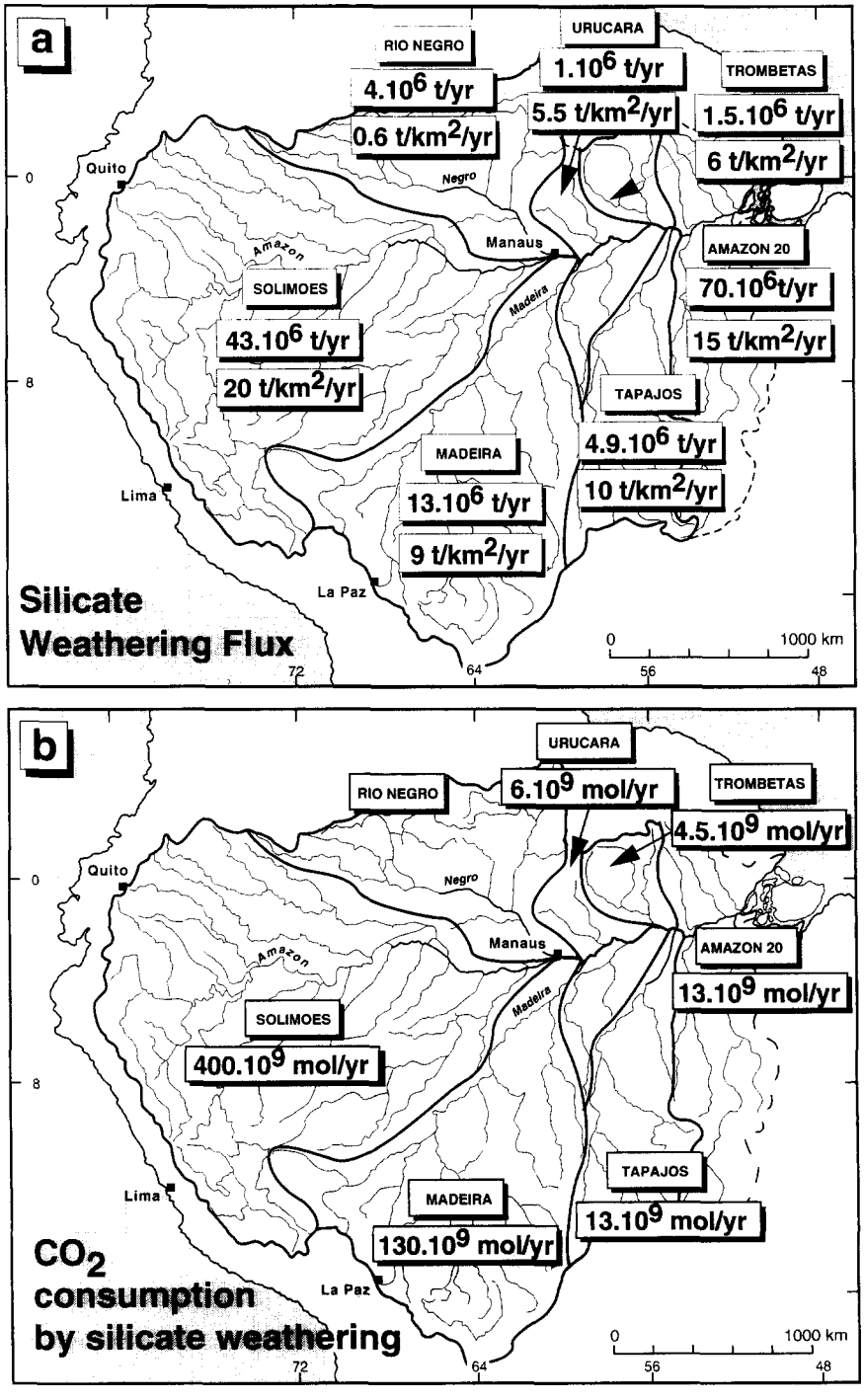

Fig. 12. Map of the Amazon Basin showing for each drainage basin (a) the chemical weathering fluxes derived from silicates, and (b) the consequent CO_2 consumption. These fluxes are calculated using the water discharge and drainage area values in Table 8. Total weathering and CO_2 consumption fluxes are given in Table 8.

Madeira tributaries, pointing out the importance of the Andes for CO_2 consumption. For comparison, the consumption in the Congo Basin is estimated to be $106 \cdot 10^9$ mol/yr (Gaillardet et al., 1995), 3 times lower than the CO_2 consumption for the Amazon Basin. The estimations are similar to those from Probst et al. (1994) based on lithologic models for carbonate weathering. For silicate weathering, the rate of CO_2 consumption is about half that of Probst et al. (1994), but in the same order of magnitude.

Finally, in Table 8 and Fig. 12, the specific weathering and CO_2 consumption fluxes are given. Due to our lack of knowledge of the carbonate and silicate outcrop areas, these rates are simply calculated using the total basin area (Table 8). They are therefore under-estimated. To bypass this difficulty, we divided the CO_2 consumption flux by the silicate weathering flux. This parameter (denoted S in Table 8) does not depend upon the silicate area. The S index ranges from 3% for the Tapajos River to 16% for the Amazon 6, and is 2 to 3 times higher in the Andean basins compared to lowland basins, highlighting the importance of the Andes in the CO_2 consumption by silicate weathering.

7. Physical weathering rates—steady-state erosion

7.1. Measured suspended sediment yields

The Amazon is probably one the most extensively documented rivers in the world for suspended sediment transport. Quantitative assessments of the transport of suspended sediments transport at different hydrological stages have been carried out for many years, in particular by the CAMREX project (e.g. Richey et al., 1986). These data provide an accurate estimate of the modern physical denudation over the drainage basin (Table 9). For the Rio Negro, Solimoes, Madeira and Amazon mainstream, the measured values are multi-year averages (1982–1984) reported by Meade (1985). The other multi-year time series (1983–1993) from Devol et al. (1995) for the Solimoes near Manaus and that (1982–1984) from Richey et al. (1986) for Solimoes, Negro, Amazon 6, Madeira and Amazon 20 are in excellent agreement with these values. All these suspended sediment concentration values have been measured for each cross-section on depth-integrated river water samples and are therefore believed by Richey et al. (1986) to be reliable estimates (to 10–20%, at the 95% confidence level) of the suspended sediments fluxes. For the other rivers (Trombetas, Tapajos and Urucara), the TSS values in Table 9 are the concentrations determined during the sampling cruise. Like the rivers of the Congo Basin (Dupré et al., 1996), these rivers are characterized by relatively small sediment yield variations during the hydrological cycle. The values measured during the sampling cruise are therefore reasonable estimates of mechanical denudation for these rivers.

These estimated mechanical denudation rates range from about 10 t km^{-2} yr^{-1} in the lowland rivers to 400 t km^{-2} yr^{-1} for the Rio Madeira Basin and lead to mechanical to chemical erosion rate ratios (mec/chem, Table 9) from 1–2 in the lowlands to 45 in the Andean basins. They point out the much larger increase of mechanical erosion compared to chemical erosion between mountains and lowlands.

The total denudation rates of silicates (τ_{sil}) are obtained by summing mechanical erosion rates and chemical erosion rates for silicates (Table 9). Expressed in mm/ka, they lead to a continental denudation close to 6 mm/ka for the lowlands rivers and between 20 and 50 mm/ka for the Andean rivers.

However, an important feature of the Andean rivers has been revealed by the PHICAB [1] program (Guyot, 1993), based on the survey of 400 streams within the Rio Madeira Basin. More than 60% of the material eroded in the Andes is deposited in the Andean piedmont (Llanos) and never leaves the drainage basin. This process is sustained by active subsidence of the Andean foreland basin. The same mechanism is most probably active for the Solimoes Basin. It has also been proposed for the Brahmaputra River (Goswani, 1985). The consequence is that the above denudation rates and mec/chem ratios (Table 9) are clearly under-estimated by a factor of 2.5 for the rivers draining the Andes.

[1] Programme Hydrologique et Climatologique du Bassin Amazonien de Bolivie (ORSTOM-SENAMHI-UMSA).

Table 9
Predicted and measured weathering rates

River	Model parameters							Measured parameters				
	α	P model		TDS_{sil}	τ_{sil}	H	mec/chem	P (TSS)		τ_{sil}	H	mec/chem
		mg/l	t/km^2/yr	t/km^2/yr	t/km^2/yr	mm/ky		mg/l	t/km^2/yr	t/km^2/yr	mm/ky	
Rio Negro	0.66±0.14	17±8	24	6	30	11	4	10	13	20	7	2
Rio Solimoes	0.704±0.10	55±26	92	21	112	42	5	226	380	400	147	19
Amazon 6	0.744±0.08	70±30	112	19	131	49	6	190	310	320	120	17
Rio Madeira	0.83±0.05	60±30	46	10	56	21	5	519	400	404	150	45
Urucara	0.88±0.05	15±7	10	6	16	6	2	8	6	11	4	1
Trombetas	0.905±0.03	7±5	7	5	9	4	1	13	11	17	6	2
Tapajos	0.90±0.05 (Na)	8±6	8	10	18	7	1	6	6	16	6	1
Amazon 20	0.86±0.06	40±25	55	16	71	26	4	230	315	330	122	21

P model is the mechanical weathering rate calculated using the model of steady-state erosion (Section 7). The P model values are calculated using Sr as the normalizing element except for the Tapajos for which Na is used. TDS_{sil} is the chemical weathering rate of silicates (Table 8). τ_{sil} is the total (chemical + mechanical) weathering rate. This rate is converted into H using a bedrock density of 2.7. Mec/chem ratio is the ratio of mechanical to chemical weathering rates.
TSS: total river suspended sediments from Meade (1985). These values are multi-year averages and determined on depth-integrated samples. They are in excellent agreement with the estimations of Richey et al. (1986) and Devol et al. (1995) for the Solimoes. TSS for the Urucara, Trompetas and Tapajos rivers have been measured at a single mid-channel point, 5 m below the surface, during the sampling cruise.

7.2. Predicted suspended sediment yields according to a steady-state model

In the following, we propose a complementary approach, based on a mass budget model, to calculate physical erosion rates. This mass budget has been initiated in the Congo Basin by Gaillardet et al. (1995). Solutes are used to calculate steady-state solid yields. In essence, the processes supplying solutes and suspended solids to the rivers (chemical and physical erosion respectively) are different. While the former acts continuously leaching the bedrock, the latter is more episodic, triggered by major flood events or mass wasting. In addition, suspended sediments are easily stored as alluvium in the river system, whereas solutes (with the exception of accumulation in saline soils) have a more conservative behaviour in the river system.

Our main purpose is to test the following mass budget for the silicate part of the continental crust:

silicate bedrocks = suspended sediments
+ dissolved silicated load

which states the steady state of weathering processes, over a given period of time. For any element X, it can then be written as $McCc(X) = MpCp(X) + MwCw^{sil}(X)$, where Mc, Mp and Mw refer to the mass of continental crust weathered during the considered period of time, the mass of suspended sediments transported and the water discharge. $Cc(X)$, $Cp(X)$ and $Cw^{sil}(X)$ are the concentrations of X in the continental crust, the suspended sediments and in the dissolved load derived from silicates, respectively. Dividing by the water discharge, Eq. 1 becomes $\tau_{sil}Cc(X) = PCp(X) + Cw^{sil}(X)$, where P, in mg/l, is the model suspended solids concentration (mechanical erosion rate) and τ_{sil} is the mass of eroded silicate continental crust per litre of water (the model total erosion rate). The mechanical and total erosion rates are related to each other by the equation $\tau_{sil} = P + 0.1P + TDS_{sil}$, where the term 0.1P accounts for the transport of continental material by the bedload sands. We assume, following previous authors (e.g. Nordin, 1985), that the transport of sediments at the bottom of the riverbeds represents 10% of the suspended transport. The parameter TDS_{sil} (total dissolved solids derived from silicates) is the chemical denudation rate (see previous section).

Practically, the model is resolved using elemental ratios normalized to Sr. The steady state is represented by a series of equations:

$$\left(\frac{X}{Sr}\right)_c = \left(\frac{X}{Sr}\right)_w \alpha + \left(\frac{X}{Sr}\right)_p (1-\alpha)$$

in which c, w and p denotes the continental crust, the dissolved load (originating from silicates) and the suspended sediments, respectively. By definition,

$$\alpha = \frac{Cw^{sil}(Sr)}{\tau_{sil}Cc(Sr)}$$

and

$$(1-\alpha) = \left(\frac{P}{\tau_{sil}} \cdot \frac{Cp(Sr)}{Cc(Sr)}\right)$$

Note that $\alpha = 1$ means that the erosion products are entirely in dissolved form, i.e. that weathering is dominated only by chemical weathering. Contrastingly, $\alpha = 0$ means a physically controlled weathering regime.

Formally, it is noteworthy that α is the same weathering index as those defined by Martin and Meybeck, 1979 (DTI: dissolved transport index, defined for any element with respect to Al) and Murnane and Stallard, 1990 and Stallard et al., 1991 (W, chemical leaching intensity, defined with respect to Si and Ge or Na, respectively).

The budget equation applies to X = Na, Ca, Rb, Ba, U and K, which are partitioned between suspended sediments and dissolved load. For the insoluble elements (Th, Ta, REE, Sc, Fe, Co, Cr, Ni), the budget equation becomes more simple:

$$\left(\frac{X}{Sr}\right)_c = \left(\frac{X}{Sr}\right)_p (1-\alpha)$$

A set of several equations is then to be solved. In the following, this set of equations is resolved by an inversion scheme similar to that developed by Gaillardet et al. (1995). In such a formalism, there are no unknowns and no data. All the equation parameters are more or less well known, the size of the error quantifying the information we have on any parameter. The parameter α and the crustal ratios are poorly known. We only know that α is a priori 0.5 ± 0.5 and particular attention has to be paid to the estima-

tion of the source rock element ratios. Because of the size of the drainage basins studied in this work, we initially assume that the continental rocks within the drainage have globally a composition close to that of the upper crust (UC) model in Taylor and McLennan (1985). If we call $Cp^*(Sr)$, the Sr concentration that suspended sediments would have if no solubilisation of this element had occurred, assuming that the local continental crust is similar to that of Taylor and McLennan's UC, then the ratio of $Cp^*(Sr)$ over Cp(Nd) is very close to the Sr/Nd ratio in the UC. In the same way, $Cp^*(Na)$, $Cp^*(Ca)$, $Cp^*(Ba)$, $Cp^*(K)$, $Cp^*(U)$, $Cp^*(Rb)$ are calculated by reference to Sm, Sc, La and Th, respectively. Graphically (Fig. 3) $Cp(Sr)/Cp^*(Sr)$ characterizes the amplitude of the negative anomaly with respect to the continental crust.

The inversion scheme has been performed for each river of this study. A-posteriori parameters are calculated. The model physical denudation rates are calculated using α and the following equation:

$$P = \frac{1-\alpha}{\alpha} \cdot \frac{Cw^{sil}(Sr)}{Cp(Sr)}$$

The results (a-posteriori values of α, P, τ_{sil}) are given in Table 9. The values of α range from 0.69 (Rio Solimoes) to 0.89 (Trombetas). The values of α for the lowlands rivers are remarkably close to the values found for the Congo rivers, indicating the similarity of their weathering regimes. By contrast, the rivers draining the Andes (Rio Solimoes, Rio Madeira and Amazon mainstream) have lower values of α.

The values of P are compared to the measured values in Table 9 and Fig. 13. Clearly, there is a discrepancy between P derived from the mass budget model and P measured in the field (TSS) for the rivers draining the Andes: Rio Solimoes, Madeira and the Amazon mainstream. The model predicted P values are 55 ± 30 mg/l and 60 ± 30 mg/l for the Solimoes and Madeira rivers respectively, while the observed values are 226 mg/l and 520 mg/l respectively. These Andean rivers thus seem to export more material than what is produced by chemical weathering in the Andes. If we take into account the accumulation of material eroded from the Andes into the Andean foreland basins, then the amplitude of the disequilibrium is even larger. By contrast, a good agreement within the uncertainties appears for the lowland rivers between P_{model} and $P_{measured}$. The same consistency is observed in the Congo Basin rivers (Fig. 13), and indicates that mechanical and physical weathering are, at the scale of the drainage basin, in steady state. The mechanical denudation is close to 10 t km^{-2} yr^{-1}, and the mechanical erosion to chemical erosion ratio is close to 1. For these rivers, the rate at which chemical weathering creates soil particles is roughly the rate at which mechanical erosion destroys the soil cover. Contrastingly, for the rivers draining the Andes, calculated mechanical denudation rates range between 50 and 110 t km^{-2} yr^{-1} and lead to mec/chem ratios close to 5. The two types of rivers highlighted by the results of this mass budget model correspond remarkably to the two types of weathering regimes recognized in the Amazon Basin by Stallard and Edmond (1987). The 'transport limited' regime characterizes the lowlands

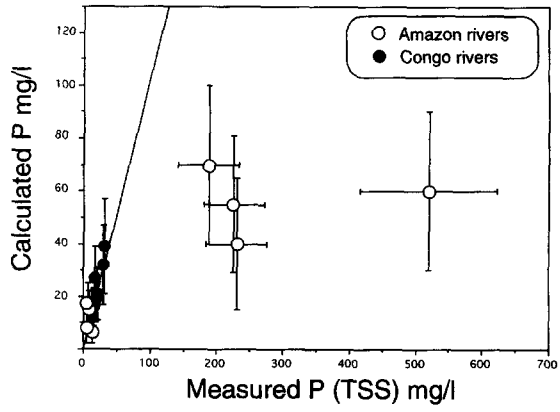

Fig. 13. Comparison between the measured values of the river suspended sediment concentration (TSS) and those calculated by the steady-state model of erosion presented in Section 7. For the rivers Solimoes, Madeira, Negro and the Amazon mainstream, the measured sediment concentrations are multiyear averages from Meade (1985) and Devol et al. (1995). For the other lowland rivers, the concentrations measured during the sampling cruise have been used. The results from the rivers of the Congo Basin have been included for comparison. What appears clearly is the discrepancy between, on the one hand, the lowland rivers of the Amazon Basin and the Congo rivers, characterized by a general agreement between predicted and observed values, and on the other hand, the rivers draining the Andes, showing observed sediment yields greater than the predicted ones. In these rivers sediment export exceeds sediment production.

rivers which have reached a steady state, while the 'weathering limited' regime characterizes the Andean rivers, which have sediment yields larger than those predicted by the steady state. The reasons for this disequilibrium are now discussed following two main directions.

7.2.1. Soil destabilization: soils equilibrium breakdown?

The result that, for the Solimoes and Madeira rivers, the predicted sediment yields are much smaller than the observed ones indicates that sediments are transported at a higher rate than the rate at which they are produced within the drainage basin. On a global scale, this means that soils are being destroyed and more precisely the soils of the Andean Cordillera, as the vast majority of suspended sediments is derived from the Andes (Allègre et al., 1996). The reason why soils in the Andean drainage basins should be in disequilibrium could be due to a recent epirogenic uplift. This process modifies the river base level. If we suppose that soils have a mean thickness close to 1 m, then at the present rate of soil destruction, 10,000 years are necessary to destroy completely the soil cover. This simple calculation is in favour of a very recently induced change.

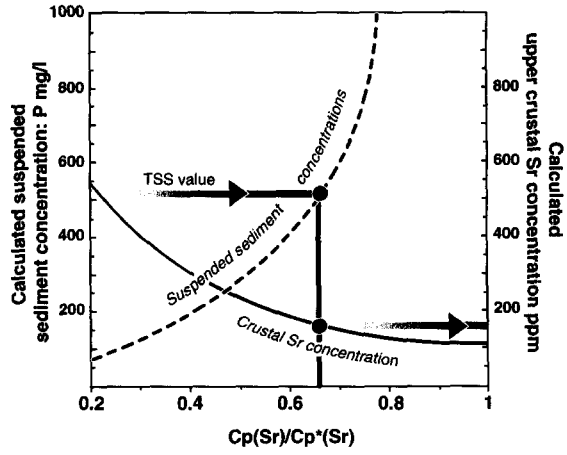

Fig. 14. Madeira River. Sensitivity test of the steady-state model described in Section 7. Using the budget equation of Sr between continental crust and river materials, these diagram describe the evolution of the predicted river sediment yield (in mg/l) and Sr concentration in the source rocks of the drainage as a function of Cp^*/Cp. Cp^* denotes the concentration that Sr would have if no solubilisation of this element had occurred. Cp^*/Cp is therefore an index of the amplitude of the Sr depletion in river suspended sediment. For the Madeira River, the multiyear average of suspended sediments is 519 mg/l (Meade, 1985). Steady-state erosion requires that $Cp/Cp^* \approx 0.65$ and therefore a source-rock Sr concentration of 150 ppm. If we consider that TSS are minimum values because of sediment storage in the Llanos plains, then Cp/Cp^* slightly increases while Cc(Sr) slightly decreases.

7.2.2. Preferential erosion of sedimentary rocks

There exists an alternative explanation for the results of the above steady-state model. The disequilibrium that we observe could be due to an incorrect estimate of the composition of the rocks undergoing weathering. In solving the model, we assumed that the a-priori crustal ratios were similar to that of the UC of Taylor and McLennan. This estimation may be erroneous because some source rocks in the drainage basin may have already experienced one or several previous erosion cycles. If so, the real crustal ratios lie somewhere between those of Taylor and McLennan and those of the sedimentary rocks (redbeds, shales, schists) from which the suspended sediments are derived. It is moreover evident that these sedimentary rocks are more sensitive to mechanical denudation than igneous rocks.

The sensitivity of the model to the composition of the rocks undergoing weathering can be tested using, for example, Sr. The mass budget equation applied to Sr gives:

$$\tau_{sil}Cc(Sr) = PCp(Sr) + C_w^{sil}(Sr) = PCp^*(Sr) \quad (1)$$

and

$$\tau_{sil} = P + 0.1S + TDS_{sil} \quad (2)$$

where $Cp^*(Sr)$ refers to the Sr concentration that the suspended load would have if no solubilisation of Sr had occurred. The variation of suspended solid concentrations P with Cp/Cp^* as well as the Sr concentration of the pristine source rocks Cc(Sr) can be then predicted. Using the TDS_{sil} and the proportions of Sr originating from silicates (Tables 7 and 8), these variations are shown Fig. 14 for the Madeira Basin. The ratio $Cp(Sr)/Cp^*(Sr) = 1$ means that the pristine rocks resemble chemically the suspended sediments. The lower limit for $Cp(Sr)/Cp^*(Sr)$ is given using the UC of Taylor and McLennan ($Cp(Sr)/Cp^*(Sr) \approx 0.2$ for the Madeira River). This

figure shows that it is possible to reconcile the measured and calculated suspended sediment concentrations in the Rio Madeira Basin, if $Cp/Cp^* = 0.6$, which corresponds to Cc(Sr) = 150 ppm. If we take into account the accumulation of suspended material in the Andean piedmont, then Cp/Cp^* is greater (for example 0.7 corresponds to TSS = 1000 mg/l), and Cc(Sr) slightly decreases (130 ppm Sr).

This calculation has been performed for all the rivers showing a discrepancy between the measured and calculated erosion rates. For the Rio Solimoes, steady-state erosion (using measured TSS) requires that Cc(Sr) = 280 ppm. For the Amazon 6 and Amazon 20, 250 ppm and 130 ppm are calculated to account for the steady state. These low concentrations compared to the Sr concentration in the granitic UC (350 ppm Sr) are consistent with the presence of a large amount of recycled source rocks having undergone previous weathering processes.

Furthermore, if we state that the above concentrations result from the mixing of pristine continental rocks close to Taylor and McLennan's UC (350 ppm Sr) and sedimentary rocks, we can then calculate the proportions of pristine continental crust and sedimentary rocks being eroded within the drainage basin. In other words, we can calculate the proportions of sedimentary recycling. For example, using the Sm/Sr ratio:

$$\left(\frac{Sm}{Sr}\right)_c = \left(\frac{Sm}{Sr}\right)_{TMcL} \gamma + \left(\frac{Sm}{Sr}\right)_{sed.} (1-\gamma)$$

where the determination of γ leads to the estimation of the mass proportion of the pristine continental crust within the drainage basin. The Sr and Sm upper crustal concentrations are determined using the above Eqs. (1) and (2). The chemical ratios of the sedimentary rocks are assumed to be those we measured in the suspended sediments of the river. Although this is quite unrealistic, it allows the calculation of the maximum percentage of pristine continental crust (and the minimum percentage of sedimentary rocks).

The results of this calculation indicate that for the Solimoes and Madeira rivers, respectively 51% and 18% of the drainage is constituted of pristine continental crust. In turn, it means that at least 56% and 18% of the mass of these drainage basin is constituted of recycled material. For the Amazon mainstream we find that 45 and 25% for Amazon 6 and Amazon 20 of the drainage basin are composed of recycled components, respectively. Finally, as the true TSS values are greater than those used in this calculation, because of the deposition of material in the foreland basin, the proportions of recycling given above are minimum values (Fig. 14).

7.3. Conclusion

This study presents a coupled geochemical investigation of major and trace elements in both suspended and dissolved materials of the Amazon River and its tributaries. The comparison of these products of physical and chemical weathering provides important constraints on the erosion and transport processes that occur at the scale of a large drainage basin as well as the fluxes of material delivered to the ocean. In particular:

– For a number of elements (e.g. REE), abnormal concentrations with regard to theoretical solubilities are observed in the dissolved phase (0.2 μm). The absolute and relative abundance (with respect to suspended load) of these elements are controlled by river pH, suggesting that colloids and (or) adsorption processes play an important role in the control of these elements.

– Conversely, the most soluble elements, such as the alkalis and alkaline-earths, are controlled by the mixing of waters from different origins: rain water, silicate weathering, carbonate and evaporite weathering. The proportions of each element derived from each source are calculated. Weathering rates of silicates are greater in the Andes compared to the lowland basins.

– Steady-state mechanical erosion rates can be calculated using a model that couples mechanical and chemical erosion. These rates can be compared to long-term measurements. In such an approach, the composition of the rock source is of critical importance. The lowland rivers correspond to the steady state, whereas the rivers of the Andes export more sediments than the amount predicted by the steady-state model. Two interpretations are then possible. Either, the rivers derived from the Andes are not in erosional steady state, and soils are being destroyed, or the disequilibrium is an artefact due to an erroneous continental crust composition being used to

solve the model. If we consider that most of the rock sources have suffered pre-depositional weathering processes (i.e. that they are recycled sediments), then it is possible to reconcile the predicted and observed mechanical erosion rates. If good estimates of the present mechanical denudation rate are available (and corrected for possible redeposition within the basin), then we can show that it is possible to calculate the proportions of pristine and recycled crust within each drainage basin. Our results show the greater importance of sedimentary recycling in young orogenic belts (Andes) compared to old cratonized shields.

Acknowledgements

This work was supported by the INSU PIRAT and DBT programs. We thank the scientists of ORSTOM (Office de Recherche Scientifique et Technique d'Outre Mer) for their technical assistance during the sampling. The Amazon sampling cruise has benefited from the help of M. Bernat, F. Seimbille, A. Chauvel (ORSTOM Manaus), A. Melphi (University of São Paolo), and Professor Abrao (Niteroi). In Paris, F. Capmas, H. Chazaly and F. Mokadem are greatly acknowledged for their analytical assistance. This paper has benefited from the constructive reviews of J.I. Drever, R.F. Stallard, J. Blum and J.L. Probst. This work was supported through the program DBT 'Fleuves et Erosion' (contribution 79). This is IPGP contribution No. 1469.

References

Allègre, C.J., Lewin, E., 1989. Chemical structure and history of the Earth: evidence from global non-linear inversion of isotopic data in a three-box model. Earth Planet. Sci. Lett. 96, 61–88.

Allègre, C.J., Hart, S.R., Minster, J.F., 1983. Chemical structure and evolution of the mantle continents determined by inversion of Nd and Sr isotopic data, I. Theoretical methods. Earth Planet. Sci. Lett. 66, 177–190.

Allègre, C.J., Dupré, B., Negrel, P., Gaillardet, J., 1996. Sr–Nd–Pb isotopes systematics in Amazon and Congo River systems. Constraints about erosion processes. Chem. Geol. 131, 93–112.

Andrae, M.O., Talbot, R.W., Berresheim, H., Beecher, K.M., 1990. Precipitation chemistry in Central Amazonia. J. Geophys. Res. 93, 16987–17000.

Berner, R.A., 1994. GEOCARB II: a revised model for atmospheric CO2 over Phanerozoic time. Am. J. Sci. 295, 491–495.

Birck, J.L., 1986. Precision K–Rb–Sr isotopic analysis: application to Rb–Sr chronology. Chem. Geol. 56, 73–83.

Degens, E.T., Kempe, S., Richey, J.E., 1991. Biogeochemistry of Major World Rivers. Wiley, New York, 356 pp.

Devol, A.H., Forsberg, B.R., Richey, J.E., Pimentel, T.P., 1995. Seasonal variation in chemical distributions in the Amazon (Solimoes) River: a multiyear time series. Global Biogeochem. Cycles 9 (3), 307–328.

Dupré, B., Gaillardet, J., Rousseau, D., Allègre, C.J., 1996. Major and trace element of river-borne material: the Congo Basin. Geochim. Cosmochim. Acta 60, 1301–1321.

Edmond, J.M., Palmer, M.R., Measures, C.I., Grant, B., Stallard, R.F., 1995. The fluvial geochemistry and denudation rate of the Guayana Shield in Venezuela, Colombia, and Brazil. Geochim. Cosmochim. Acta 59, 3301–3325.

Elderfield, H., Upstill-Goddard, R., Sholkovitz, E.R., 1990. The rare earth element in rivers, estuaries, and coastal seas and their significance to the composition of ocean waters. Geochim. Cosmochim. Acta 54, 971–991.

Ferreira, J.R., Devol, A.H., Martinelli, L.A., Forsberg, B.R., Victoria, R.L., Richey, J.E., Mortatti, J., 1988. Chemical composition of the Madeira River: seasonal trends and total transport. In: Transport of Carbon and Minerals in Major World Rivers. Mitt. Geol. Paläontol. Inst. Univ. Hambourg, SCOPE/UNEP Sonderband (66), pp. 63–75.

Forti, M.C., Moreira-Nordemann, L.M., 1991. Rainwater and troughfall chemistry in a 'Terra Firme' rain forest: Central Amazonia. J. Geophys. Res. 96 (D4), 7415–7421.

Furch, K., 1984. Water chemistry of the Amazon Basin: the distribution of elements among freshwaters. In: The Amazon. Monogr. Biol. 56, 127–167.

Gaillardet, J., Dupré, B., Allègre, C.J., 1995. A geochemical mass budget model applied to the Congo Basin Rivers. Erosion rates and composition of the continental crust. Geochim. Cosmochim. Acta 59, 3469–3485.

Galloway, J.N., Likens, G.E., Keene, W.C., Miller, J.M., 1982. The composition of precipitation in remote areas of the world. J. Geophys. Res. 96 (D4), 7415–7421.

Garrels, R.M., MacKenzie, F.T., 1971. Evolution of Sedimentary Rocks. Norton, New York.

Gibbs, R.J., 1967. The geochemistry of the Amazon River system. The factors that control the salinity, composition and concentration of the suspended solids. Geol. Soc. Am. Bull. 78, 1203–1232.

Gislason, S.G., Arnorsson, S., Armannsson, H., 1996. Chemical weathering of basalt in SW Iceland: effects of runoff, age of rocks and vegetative/glacial cover. Am. J. Sci. 296, 837–907.

Goldstein, S.J., Jacobsen, S.B., 1987. The Nd and Sr isotopic systematics of river-water dissolved material: implications for the sources of Nd and Sr in seawater. Chem. Geol. 66, 245–272.

Goldstein, S.J., Jacobsen, S.B., 1988a. Nd and Sr isotopic systematics of river-water suspended material: implications for crustal evolution. Chem. Geol. 87, 249–265.

Goldstein, S.J., Jacobsen, S.B., 1988b. Rare earth element in river waters. Earth Planet. Sci. Lett. 89, 35–47.

Goswani, D.C., 1985. Brahmaputra river, Assam, India: physiog-

raphy, basin denudation and channel aggradation. Water Resour. Res. 21 (7), 959–978.

Guyot, J.L., 1993. Hydrogéochimie des fleuves de l'Amazonie bolivienne. Thèse Université Bordeaux I, Editions de l'ORSTOM, Paris.

Hofmann, A.W., 1988. Chemical differentiation of the earth: the relationship between mantle, continental crust and oceanic crust. Earth Planet. Sci. Lett. 90, 297–314.

Irion, G., 1983. Clay mineralogy of the suspended load of the Amazon and the rivers in the Papua–New Guinea mainland. In: Transport of Carbon and Minerals in Major World Rivers. Mitt. Geol. Paläontol. Inst. Univ. Hamburg, SCOPE/UNEP Sonderband (55), pp. 483–504.

Keasler, K.M., Loveland, W.D., 1982. Rare earth elemental concentrations in some Pacific Northwest Rivers. Earth Planet. Sci. Lett. 61, 68–72.

Konhauser, K.O., Fyfe, W.S., Kronberg, B.I., 1994. Multi-element chemistry of some Amazonian waters and soils. Chem. Geol. 111, 155–175.

Kronberg, B.I., Nesbitt, H.W., Fyfe, W.S., 1987. Mobilities of alkalies, alkaline earths and halogen during weathering. Chem. Geol. 60, 41–49.

Langmuir, D., Herman, J.S., 1980. The mobility of Th in natural waters at low temperatures. Geochim. Cosmochim. Acta 44, 1753–1766.

Lesack, L.F.W., Melack, J.M., 1991. The deposition, composition and potential sources of major ionic solutes in rain of the Central Amazon Basin. Water Resour. Res. 27 (11), 2953–2977.

Louvat, P., Allègre, C.J., 1997. Denudation rates at Reunion Island determined by river geochemistry: basalt weathering and mass budget between chemical and mechanical erosions. Geochim. Cosmochim. Acta (in press).

Martin, J.M., Meybeck, M., 1979. Element mass-balance of material carried by major world rivers. Mar. Chem. 7, 173–206.

Martin, J.M., Whitfield, M., 1983. The significance of the river input of chemical elements to the ocean. In: Trace Metals in Sea Water. Plenum Press, London, pp. 265–296

Meade, R.H., 1985. Suspended sediment in the Amazon river and its tributaries in Brazil during 1982–1984. U.S. Geol. Surv. Open-File Rep. 85 (492), 1–40.

Meybeck, M., 1983. Atmospheric inputs and river transport of dissolved substances. Proc. Hamburg Symp., IAHS Publ. 141.

Meybeck, M., 1986. Composition chimique des ruisseaux non pollués de France. Sci. Geol. Bull. 39 (1), 3–77.

Meybeck, M., 1987. Global chemical weathering from surficial rocks estimated from river dissolved loads. Am. J. Sci. 287, 401–428.

Molinier, M., Guyot, J.L., De Oliveira, E., Guimaraes, V., Chaves, A., 1993. Hydrologie de Bassin de l'Amazone. In: Grands Bassins Fluviaux Périatlantiques. Proceedings of the PEGI-INSU-CNRS-ORSTOM Symposium. Orstom Editions, Paris, pp. 335–345.

Murnane, R.J., Stallard, R.J., 1990. Germanium and silicon in rivers of the Orinoco drainage basin. Nature 344, 749–752.

Négrel, P., Allègre, C.J., Dupré, B., Lewin, E., 1993. Erosion sources determined by inversion of major and trace element ratios in river water: the Congo Basin case. Earth Planet. Sci. Lett. 120, 59–76.

Nesbitt, H.W., Markovics, G., Price, R.C., 1980. Chemical processes affecting alkalis and alkaline earths during continental weathering. Geochim. Cosmochim. Acta 44, 1659–1666.

Nordin, C.F. Jr., 1985. The sediment load of rivers. In: Rodda, J.C. (Ed.), Facets of Hydrology. Wiley, New York, pp. 183–204.

Palmer, M.R., Edmond, J.M., 1992. Controls over the strontium isotopic composition of river water. Geochim. Cosmochim. Acta 56, 2099–2112.

Palmer, M.R., Edmond, J.M., 1993. Uranium in river waters. Geochim. Cosmochim. Acta 57, 4947–4955.

Probst, J.L., Nkounkou, R.R., Krempp, G., Bricquet, J.P., Thiebaux, J.P., Olivry, J.C., 1992. Dissolved major elements exported by the Congo and the Ubangui rivers during the period 1987–1989. J. Hydrol. 135, 237–257.

Probst, J.L., Mortatti, J., Tardy, Y., 1994. Carbon river fluxes and weathering CO_2 consumption in the Congo and Amazon river basins. Appl. Geochem. 9, 1–13.

Richey, J.E., Meade, R.H., Salati, E., Devol, A.H., Nordin, C.F. Jr., Dos Santos, U., 1986. Water discharge and suspended sediment concentrations in the Amazon River: 1982–1984. Water Resour. Res. 2 (5), 756–764.

Salati, E., Marques, J., 1984. Climatology of the Amazon Region. In: The Amazon. Monogr. Biol. 56, 47–85.

Schindler, P.W., Stumm, W. (Ed.), 1987. Aquatic Surface Chemistry. Wiley-Interscience, New York.

Sholkovitz, E.R., 1992. Chemical evolution of rare earth elements: fractionation between colloidal and solution phases of filtered river water. Earth Planet. Sci. Lett. 114, 77–84.

Sholkovitz, E.R., 1995. The aquatic chemistry of rare earth elements in rivers and estuaries. Aquat. Geochem. 1, 1–34.

Sioli, H., 1984. The Amazon and its main afluents: hydrography, morphology, river courses and river types. In: The Amazon . Monogr. Biol. 56, 85–127.

Soler, P., Rotach-Toulhoat, N., 1990. Implication of the time-dependent evolution of Pb-and Sr isotopic compositions of Cretaceous and Cenozoic granitoids from the coastal region and the lower Pacific slope of the Andes of central Peru. Geol. Soc. Am., Spec. Pap. 241, 161–172.

Stallard, R.F., 1980. Major Element Chemistry of the Amazon River System. Ph.D. dissertation, MIT/WHOI.

Stallard, R.F., 1995a. Tectonic, environmental and human aspects of weathering and erosion: a global review using a steady-state perspective. Annu. Rev. Earth Planet. Sci. 23, 11–39.

Stallard, R.F., 1995b. Relating chemical and physical erosion. In: White, A.F., Brantley, S.L. (Eds.), Reviews in Mineralogy, 31. Mineralog. Soc. Am., pp. 543–564.

Stallard, R.F., Edmond, J.M., 1983. Geochemistry of the Amazon, 2. The influence of geology and weathering environment on the dissolved load. J. Geophys. Res. 88, 9671–9688.

Stallard, R.F., Edmond, J.M., 1987. Geochemistry of the Amazon, 3. Weathering chemistry and limits to dissolved inputs. J. Geophys. Res. 92, 8293–8302.

Stallard, R.F., Koehnken, L., Johnsson, M.J., 1991. Weathering processes and the composition of inorganic material trans-

ported through the Orinoco River system, Venezuela and Columbia. Geoderma 51, 133–165.

Taylor, S.R., McLennan, S.M., 1985. The Continental Crust: Its Composition and Evolution. Blackwell, Oxford, 312 pp.

Trimble, W.S., 1977. The fallacy of the stream equilibrium in contemporary denudation studies. Am. J. Sci. 277, 876–887.

Viers, J., Dupré, B., Polvé, M., Schott, J., Dandurand, J.L., Braun, J.J., 1997. Chemical weathering in the drainage basin of a tropical watershed (Nsimi–Zoetele site, Cameroon): comparison between organic poor and organic rich waters. Chem. Geol. (in press).

Whitfield, M., Turner, D.R., 1979. Water–rock partition coefficients and the composition of sea water and river water. Nature 278, 132–137.